LUNDS UNIVERSITET

FACULTY OF ENGINEERING, LTH
DEPARTMENT OF MECHANICAL ENGINEERING SCIENCES

Adhesive bonding of fiber laminate patch to sandwich-structured composite

Supervisor:
Prof. Dmytro Orlov
Co-Supervisor:
Tomas Rommer
Examiner:
Per Hansson

Author:
Daniel Nesic
danielnesic@yahoo.se

THESIS FOR THE DEGREE OF MASTER OF SCIENCE

Project duration: January 2022 - June 2022

MSc Thesis
ISBN LUTFD2/TFMT--22/5067--SE
Division of Materials Engineering
Department Mechanical Engineering
Lund University
Box 118
SE-22100 Lund
Sweden

Printed in Sweden
Lund 2022

Abstract

By using composites when constructing vehicles, lighter weight and thus better performance can be achieved. Composites are widely used in airplanes and small boats, but has yet to be incorporated in larger ships such as freighters and cruise ships. The main hindrance for its use is the lack of practical knowledge and experience. However, the Visby corvette is a 70 m ship made entirely out of composite and a great proof of concept. The Visby is made by Saab Kockums which also uses composites in many other of their products and continually seeks improvements. One such improvement can be made in joining techniques by attaching composite structures with an adhesive. However, predicting the load bearing capability of adhesive joints proved difficult. Therefore, a literature survey has been carried out to find the most important parameters for the load bearing capability of the adhesively attached patch. After this investigation it was decided that stress concentrations arising in the adhesive joint should be investigated with finite element (FE) methods and confirmed with optical microscope images of patches that had already been mechanically tested. FE modeling succeeded in predicting failure in accordance with the adhesive joints that were modeled. The microscope images confirmed the results from the FE modeling, but also revealed areas of failure in the adhesive joint which could not be predicted with the FE models. Improvements for the FE model were also discussed to facilitate its use when constructing composite structures. A better model would aid in expanding the use of composites and reaping the benefits of those materials.

Populärvetenskaplig sammanfattning

Saker som ska röra sig har ofta stor fördel av att vara lätta, då detta minskar energin som krävs för att få dem att röra sig och eller ökar deras topphastighet. Detta har flitigt använts inom flygindustrin där strikta krav ställs på flygplan vad gäller nyttolast och bränsleförbrukning. En stor del i detta utvecklingsarbete har bestått i att ändra eller förbättra materialen som flygplan byggs i. Denna materialutveckling har även skett bland båtar som gått från att byggas i trä, till smidesjärn och sedan stål. Här blev emellertid resultatet att båtar kunde byggas mycket större snarare än att de blev lättare även om det ofta också var fallet.

Dagens Flygplan är till stor del byggda av kompositmaterial och deras styrka, styvhet och låga vikt har bidragit till att öka flygplanens prestanda. I takt med att dessa material blir billigare och att kunskapen om dem ökar blir möjligheten att använda dem till bilar och båtar allt större.

Dock låter kanske inte komposit så nytt för båtentustiasten som redan har en glasfiberbåt i garaget. Men i stora lastfartyg eller i stora kryssningsfartyg används i princip kompositer aldrig som byggnadsmaterial. Trots detta kan den lägre skeppsvikten som kommer av att bygga i komposit leda till fördelar som högre hastighet, lägre bränsleförbrukning och ökad stabilitet. Det som står i vägen för dessa fördelar är potentiellt för låg styvhet för vissa applikationer, potentiellt höga kostnader och avsaknad av storskaliga produktionsanläggningar. Framförallt är det dock avsaknad av erfarenhet på området som saknas. Skeppsbygge är en väldigt gammal kunskap som utvecklats över lång tid för att lyckas inse alla möjligheter och undvika alla fallgropar. Därför är materialbyte inte något som görs på en dag, särskilt inte när man byter från stål till kompositer vilka är väldigt olika material.

Ett skepp som dock ligger i framkant när det gäller att använda kompositer är Visbykorvetten som är över 70 m långt helt gjord i kolfiberkomposit vilket ger den halva vikten jämfört med ett stålskepp i samma storlek. Kockums, företaget som tillverkat Visby, använder även kompositer till radarmaster och skeppsöverbyggnader som de tillverkar och moderbolaget Saab använder kompositer till deras flygplan. Därför finns det ett stort intresse av att förbättra förmågan att bygga med kompositer. Ett potentiellt sätt att göra detta på är genom att använda mer limförband mellan kompositdelar istället för skruvförband med håltagning och stålinsatser ingjutna i kompositstrukturen. Genom teknikskiftet kan ett lättare och starkare förband fås som dessutom går att flytta eller modifiera utan att reparation av hål i strukturen krävs.

I denna rapport undersöks relevanta parametrar för bärförmågan i denna nya typ av limfog genom att studera litteratur på området. Bland dessa parametrar finns frågan om ifall limmet som används är rätt för uppgiften, om det kemiskt kan

försvaga härdplasten som håller ihop kolfibrerna och vilken tjocklek man bör ha på limfogen. Litteraturstudien kompletteras med en mer noggrann undersökning av fästpunktens utformning eller snarare hur denna utformning orsakar en ojämn lastfördelning i limfogen. Undersökningen av limfogen görs med hjälp av finita element metoder, ett kraftfullt verktyg där stora föremål som normalt hade behövt beskrivas av komplicerade differentialekvationer delas upp i ett stort antal små delar. Dessa delarna kan beskrivas med mycket simplare ekvationer som sedan summeras och används för att approximera det mer komplicerade problemet, en uppgift som är perfekt för en dator. Finita element metoderna kompletteras med optisk mikroskopering för att kunna verifiera dessa beräkningar och för att hitta saker som den mer snäva finita element metoden skulle kunna missa. Finita element metoden och mikroskoperingen ger samma resultat nämligen att det är kolfibret som går sönder först när limfogen belastas till den brister.

Med fortsatt förfining och optimeringen av den finita element metoden som använts kan limning som fästmetod bli mer vanlig. Detta kan sedan leda till att komposit används i större utsträckning för att bygga fordon av alla slag som då kan bli snabbare och mer bränslesnåla.

Acknowledgements

Firstly, I would like to thank my supervisor Dmytro Orlov for supporting me with my thesis from before it had even begun and until the end. He has also been very generous with his time and could be reached by email on any and all times. Furthermore, he provided me with valuable feedback that mixed praise with constructive criticism and he understood that I had a learning curve in front of me and that everything wouldn't be right the first time.

Secondly, I would like to thank my co-supervisor Tomas Rommer for being a very calm and patient teacher while refreshing and improving my finite element modeling skills. He also created the original 70 mm FE model which much of the FE work in this report is based on. It has also been very nice working with him because of his flexibility and the time he devoted to me and my thesis project. Lastly, I would also like to thank both him and his family for inviting me to his home while I visited Karlskrona.

Thirdly, I would like to thank Hans Forsman for helping me with practical material questions, sample preparation, for showing me around the composite workshop and for participating in all of the meetings with Dmytro, Tomas and me.

Another thanks goes to the members of Dmytro's seminar group for giving me valuable feedback on how to properly present my report and for helping me in the lab.

Lastly, I would like to thank my family and friends for their general support and encouragement. I also want to give my friends extra thanks for giving me tips on how to structure my report, helping me with LaTeX and of course for helping me with my CV which ultimately enabled me to write this thesis work.

Table of Contents

1 Introduction

Ships have been a very important mode of transportation to humans for a very long time. Especially in the early days of civilization boats were the only mode of transportation that could reach remote locations and throughout history ships have been the mode of transportation with the highest weight and volume capacity.

However, the ships we operate have come a long way in their development during the thousand years we sailed them. In the beginning ships could only travel on rivers and calm waters closer to shore, but with better and larger ships, humans could eventually sail all over the world. Nevertheless, even though the ships became better and larger some things still remained the same, such as the early propulsion modes consisting primarily of sails and oars. Another thing that has remained fairly constant through history is the building material of ships being wood. Wood has a fairly good specific strength, is naturally buoyant and is easy to work with so its use in shipbuilding is a given. [1] [2]

Nonetheless, with the industrial revolution humans gained access to many new technologies such as steam engines and screw propellers, but also new materials like wrought iron and eventually steel.[3][4][5] At the same time the limitations of wood in shipbuilding were discovered when very long ships, over 90 m, experienced excessive flexing which caused leakage and unacceptable stress at joints.[6] The reason for this problem was insufficient structural stiffness. So, at the end of the 1800s there was finally a shift in the main material being used for ships from wood to wrought iron and eventually steel, at least in large commercial and military ships.

The need for stiff and strong materials is not unique for shipbuilding, but is a necessity in all modes of transportation. However, airplanes in particular have a very high demand for strong and stiff materials that are also lightweight. So much like ships they were first built out of wood, but then moved on to metals. But the evolution of airplanes did not stop at metals and modern aircraft are to a large extent built out of fiber reinforced composites.[7][8]

Today the use of fiber reinforced composites is also very prevalent in small ships, but have not gained traction among larger ships despite the advantages they promise.[9] Nevertheless, exceptions exist, such as the Visby class corvette which is one of the largest ships entirely made out of fiber composites. The Visby corvette is a military ship, but it is not uncommon for military technologies to lead the way in technological innovations. These innovations can then eventually find their way to the civil sector and can thus benefit the larger population. [9]

By using fiber composites in shipbuilding some advantages can be achieved in-

cluding lighter weight, which can lead to better fuel economy or higher speed and increased stability by reducing top weight of ships. [9] Fiber composites could also lead to less maintenance and maintenance related cost because of less corrosion compared to steel. Moreover, if produced in large quantities they can even prove to reduce production costs compared with metal hulled ships. Nevertheless, if sufficient quantities aren't reached or if high performance composites are used the production costs instead increase. However, even greater disadvantages exist, such as the lack of experience in building large composite ships. It is also harder to produce composite ships with sufficient fire safety and there are few shipyards that are capable of repairing large scale composite ships. [9]

So composites are a promising material for use in basically all vehicles. Nonetheless, composites have a more complex behavior than metals because they are anisotropic and because it is a newer material there is less experience working with it. A small step towards improving the knowledge on the subject and making composites easier to use can be taken by improving joining technologies. This is something that Saab Kockums are investigating to improve their different composite structures. The technique uses a glass fiber patch containing a bolt thread and that is then adhesively attached to the ship's hull, this can be seen in figures, 1a and 1b.

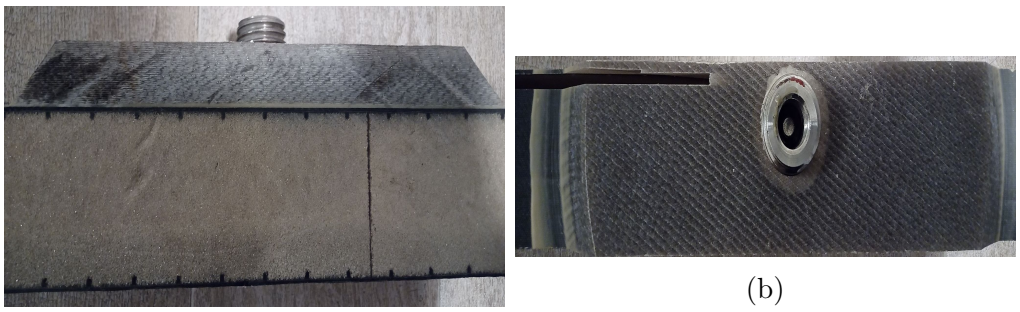

(a) (b)

Fig. 1: (a) Cross section of a hull piece with a patch attached to it. (b) Top view.

Steel inserts and bolt threads have previously been attached by drilling holes in the ship's hull and moulding them in place with a plastic filler. The main downsides of this technique is that holes needs to be drilled in the hull panel and the that the steel inserts needs to be molded in place. The holes in the hull panel also adds considerable repair work if the attached equipment is to be removed or relocated. On the other hand, there is little experience with using patches fastened with adhesives and it is hard to determine the strength of an adhesive bond without mechanically testing it. Nevertheless, manufacturing samples for testing adhesive joints is expensive and time consuming. So, to help ship designers choose a patch

with the correct load bearing capacity Kockums want to develop a set of tools to predict the performance of different patch sizes. If successfully implemented these tools could reduce the need for mechanical testing saving time and resources.

The main goals of this thesis project is therefore to:

- To build a finite element model to predict load bearing capability of adhesive joints between a glass fibre patch and a carbon fiber sandwich panel.
- Formulate recommendations for the designers of adhesive joints in ship building at Kockums

This thesis project aims to achieve its goals by:

1. Identifying critical parameters to control the load bearing of the adhesive joint.
2. Carrying out fractography analysis of adhesive joints after mechanical testing at.
3. To validate the developed finite element model with fractography results.

2 Revealing critical parameters for the load bearing capability of the adhesive joint

This project report begins by revealing critical load bearing parameters for the adhesive joint. This is done to focus time and resources. First, relevant background information together with potentially critical parameters will be presented. The parameters that are believed to be important are; strain rate, adhesive thickness, aging and environmental resistance, compatibility between the adhesive and the adherents and finally the size and geometry of the patch. After each parameter a short summary will follow and at the end of the chapter a complete summary on how to proceed with all the parameters will be presented.

2.1 Composite materials

A composite material consists of two or more different substances with varying properties which are combined to create a new material.[10][11] The substances that constitute the composite remain distinct and retain their own material properties. However, on a macroscopic scale the individual substances interact to create a material with much different and in many ways superior properties compared with the constituents. Examples of composite materials include concrete where gravel is contained within the cement, a mud brick containing straw or ceramic fibers contained within the bulk of another ceramic.[11]

In a composite material the different constituents can be classified into two main groups; the matrix and the reinforcement.[10] In the case of concrete the reinforcement is the large gravel particles, but when the reinforcement consists of fibers the composite is instead called a fiber reinforced composite or fiber composite for short. The fibers in a fiber composite often possess incredible properties when it comes to tensile strength (TS) and modulus, but has virtually no compressive strength.[12] So by embedding the fibers in a matrix they can be protected from chemical and physical damage and also gain compressive strength from the matrix and from the way the fibers interact in and with the matrix. To approximate the properties of the fiber composite in the direction parallel with the fibers the rule of mixtures can be used.[13] These properties can be calculated as the sum of the volume fractions of the two constituents multiplied with their respective property values (see equation 1).

$$x_c = x_f V_f + x_m V_m \tag{1}$$

In the above equation x_c is the property x of the composite such as its tensile strength. $x_f V$ is the same property x of a pure fiber multiplied with its volume

fraction V_f. Lastly, $x_m V_m$ is the property x of the matrix multiplied with its volume fraction V_m

One of the most common fiber composites is glass fiber reinforced composite (GFRP).[14] GFRP is actually a group of different materials where the matrix, fibers and fiber arrangement can be varied. Nonetheless, the matrix is often a plastic and often of the thermosetting type because it can easily be molded with little heat.[15] In some more advanced or demanding applications the glass fibres can be replaced by carbon fibers creating Carbon Fiber Reinforced Plastic (CFRP) which have higher tensile strength and modulus and also higher specific tensile strength and modulus.[12][1]

Both GFRP and CFRP have very high specific strength and stiffness compared to normal bulk materials such as steel and aluminum.[1] However, they are anisotropic which means special care has to be taken when designing structures made out of these materials to make sure they are loaded in the direction they are strongest. Although, this anisotropy can be somewhat mitigated by constructing the composite in a layered structure known as a laminate which can be seen in figure 2.[16] By constructing the composite as a laminate, laminae with varying fiber directions can be stacked in alternating patterns to create a more isotropic material.[17] Despite the laminar structure composite materials still tend to fail in a brittle manner, and laminates are also sensitive to delamination, which is a separation of the different laminae.[18] Delamination generally happens because of the low strength of the matrix compared to the reinforcing fibers. Additionally, composites also tend to be rather expensive. So it is these pros and cons that need to be considered when working with composite materials and the complexities that arise from the above mentioned properties is what partly necessitates and justifies the existence of this project.

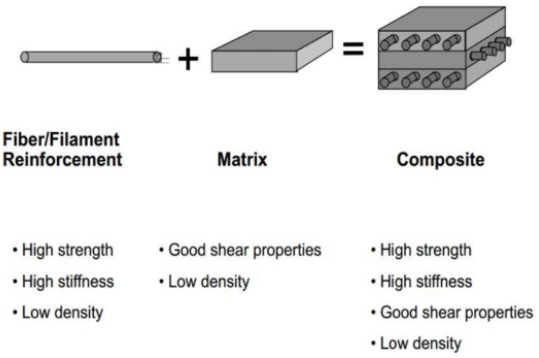

Fig. 2: The basic structure of many fiber composites. The fibers are embedded in a matrix and form one layer or lamellae and these layers are then combined to form a laminate. In the laminate shown in this image the fibers alternate their directions from 0 to 90 degrees between each layer, this is done to give the laminate more uniform mechanical properties. [19]

Composite materials that can be considered even more complex are sandwich-structured composites. A sandwich-structured composite is a composite made up of 3 layers, two thin but strong sheets on the outside and a lightweight core.[20] Thus, the materials that make up the sandwich composite is even more distinct compared with fibre composites. The idea behind a sandwich composite is that the thin, strong and stiff skins will carry tension and compression loads while the thick and lightweight core provide spacing for the skins and carry shear loads. The core can also provide great acoustic and thermal insulation. Because of its structure, sandwich composites can achieve 7 times the stiffness and 3.5 times the flexural strength by doubling the core thickness while only gaining 3 percent in total weight.[7]

Furthermore, its important to note that sandwich composites just like fibre composites can be tailored to many different tasks. To begin with there are many core structures such as foam, honeycomb or corrugated core and these cores can be made out of different materials like plastic, aluminum or steel.[7][20] A better understanding of the appearance of the different cores can be seen in figure 3. The skins can also be made of different materials like wood, steel or fibre composite and the relative thickness of the skins compared to the core can be varied and the front and back skins can have different thicknesses. With these design considerations one can achieve much varied performance that suits different purposes. For example, in a small sofa table the “strong” skins might be higher quality cardboard with the core consisting of a honeycomb structure of cardboard, but when making a military aircraft the skins might be CFRP with an aluminum honeycomb structure. The relative performance of different cores made of different materials can be seen

in fig 4.

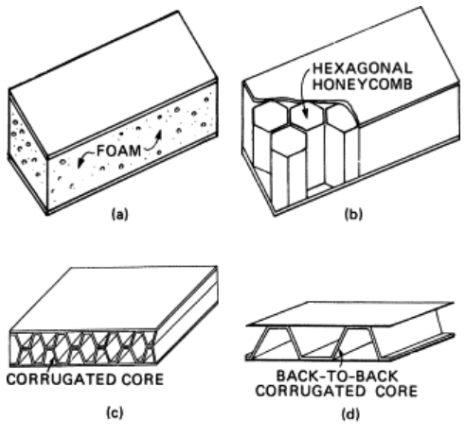

Fig. 3: Four different types of cores for sandwich panels.[20]

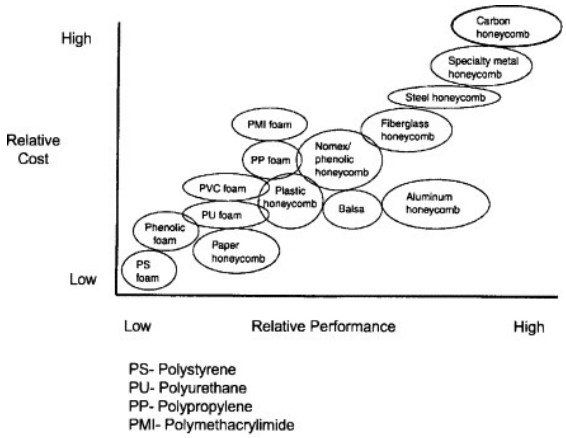

Fig. 4: The relative cost vs relative performance for different core materials.[7]

The tailoring of the sandwich composite to whatever needs one has brings up one of the downsides with sandwich composites which is their complexity. This applies to everything from their design, to computer modeling and the actual construction. This complexity is compounded when advanced materials such as fibre composites are used to create the sandwich composite. Moreover, as with most high performing materials, sandwich composites tend to be very expensive especially the sandwich composites that are used for air and spacecraft.[9] Nonetheless, major developments are being made which can reduce the costs and therefore cause sandwich composites to be relevant for more applications such as large naval ships[9]

2.2 Joining of materials

2.2.1 Joining techniques from bolts to adhesives

When constructing any object especially large and complex ones it can be hard to manufacture them as a single piece. So they are instead made in parts that need to be assembled to make the finished object. When the parts are joined they need to be kept together in some way, and how the parts are kept together depends on the requirements of the finished product. Therefore, a large number of different joining techniques with their own advantages and disadvantages exists.

On the most basic level joining techniques can be divided into two types based on what type of bond the joint creates. These types are mechanical joining and bonding on an atomic or molecular level. Mechanical joining as the name suggests joins two parts with the aid of mechanical interference and interlocking. Examples of mechanical joining techniques include, but are not limited to bolting, riveting, screwing and clinching. [21]

Atomic and molecular bonding could be considered to be more varied and specialized compared with mechanical joining, because they include techniques such as fusion welding, soldering, friction welding and adhesive bonding. Some of these techniques such as fusion welding and soldering destroy adherents that can't handle the heat of the molten metal. On the other hand, mechanical joining techniques such as bolting can technically be used for attaching two pieces of cardboard as well as two steel plates. So considering its very unspecific nature and its simplicity it is not strange that bolting is such a common technique. [21]

Nonetheless, as with most general approaches they are rarely the best option for a task, even though they work fairly well. Some downsides of bolting are added weight, stress concentration at the bolting site due to the small bonding area and bad insulation of vibrations, sound and electricity (contact corrosion). Finally, the rather large holes that are needed when bolting is especially detrimental for fiber composites. Holes in materials always affects their structural integrity, but when it comes to fiber composites holes damage the fibres which can stretch beyond the site of the actual hole. Moreover, the stress concentrations at the bolting site combined with the damaged fibres, the exposed edges of the lamellae and potential damage such as cracks means there is a risk of delamination. The delamination can then spread from the site of the hole to affect more of the composite. [7]

To combat these limitations one can employ adhesive bonding. Adhesive bonding is the use of a polymeric material both thermosetting or thermoplastic to join materials by bonding to them with different mechanisms while hardening through curing or cooling from a melt. Adhesive bonding most often results in weight

savings because only a thin layer of a lightweight (compared to metals) plastic is required to join materials. Furthermore, the bonding can take place over a very large area which then gives rise to a stiffer bond with less stress concentrations. However, adhesive bonding also has disadvantages, such as requiring considerable time to harden and achieve adequate bond strength. Difficulties in disassembling the joint without damaging the adherents. Additionally, surface preparation is more important when creating an adhesive joint if proper strength is to be achieved. [7]

Nonetheless, the most important disadvantage for this report is that an adhesive joint cannot be fully tested without destructive methods. Destructive tests require more time and resources and is thus a limitation in the design of a potential joint. So that is one of the reasons why FE methods will be used to achieve the goals of this thesis, to reduce the amount of testing and to help in revealing mechanisms that causes failure in the adhesive joint. [21]

2.2.2 Adhesive bonding mechanisms

How adhesive bonding works is not fully understood, but there is a number of theories or factors that play a crucial part depending on the adherents and the adhesive used. Some of these theories are presented below.

One of these theories is that adhesives create a bonded joint through mechanical interlocking. So while the adhesive is less viscous it can enter into small crevices and ridges on the surface of the adherent which are present due to surface roughness of the material. Then, after hardening the adhesive will be unable to exit the crevices unless a rather large amount of force is used to deform or break the adhesive in order to separate the adherents. This theory is supported by the fact that most adhesives require a lot of surface preparation like, mechanical abrasion or chemical pickling to achieve greater strength in the joint. However, the increase in bond strength caused by the surface roughness could also be due to other potential mechanisms which will be explained below. Another theory proposes that adhesion is created by the inter diffusion of the adherents. This theory would be most relevant for polymers, where it is believed that a boundary layer is created and in this layer polymer chains from different adherents could intertwine to create strong adhesion. Nonetheless, polymers usually have poor solubility in other polymers unless they are chemically very similar, so the general applicability of this theory might be limited. [22]

A third theory suggests that adhesion is caused by secondary molecular interactions such as London dispersion forces and hydrogen bonding. Although these surface forces might play a part in adhesive bonding they are not strong enough to

solely explain the strength achieved in many adhesive joints. Chemical reactions is also a proposed explanation to adhesion phenomena. Just as the diffusion theory this mechanism might not be generally applicable, but in special cases is definitely something to consider. [22]

Furthermore, electrostatic forces are believed to play a part in the strength of adhesive joints. Electrostatic forces that arise in this case is due to the assumption that electrons would occupy different energy levels on the two different adherents which would facilitate electron transport when they come in contact. The following charge imbalance would then cause the attraction between two surfaces. However, it is worth to mention that the electrostatic force just like the secondary molecular interactions is only believed to play a minor part in most adhesive joints. The last theory regarding adhesion is one based on acids and bases. This theory can be used both with the Bronsted and the Lewis definition of acids and bases. According to the later and more general definition by Lewis an acid is a substance that can accept an electron pair and a base is a substance that can donate an electron pair. So this theory states that adhesion can be established because of the polar attraction of Lewis acids and bases or in other words between electron poor and electron rich substances. [22] [23]

Additionally, an aspect that might be important to all of the above theories is wetting. Wetting is the tendency of a liquid to spread out on a surface or to bunch up into a sphere. Wetting is affected by the surface, the liquid and the atmosphere surrounding them both and the liquids behavior in spreading out or not serves to minimize surface energy. Wetting is important because if the liquid or in this case the adhesive has a tendency to spread out on the surface that means that it can better fill up holes and gaps on the surface. This is important because many of the effects above rely on a close distance and a good interface between the adhesive and adherent to form a strong bond. [22]

2.2.3 Aging and environmental resistance

Just as adhesion involve both chemical and physical aspects so does aging and environmental resistance. Aging and environmental resistance is yet another parameter that is believed to be crucial for the load bearing capability of the joint. A lot of tests related to this parameter have already been done by Huntsman (the manufacturers of the adhesive used to attach the patch). In these tests the adhesive (Araldite 2015-1) have been exposed to different liquids and conditions and these can be seen in figures 5 and 6. According to these tests many of the tested chemicals didn't seem to cause any significant reduction in the strength of the adhesive with a few exceptions. However, as long as these exceptions are not something that is readily encountered, then the chemical or environmental resis-

tance of the adhesive is not a problem. Nonetheless, something that seemed to be lacking in the tests is the effects of saltwater on the adhesive, which might often be encountered on a ship. Therefore, a literature survey was conducted. The findings however are only general because they are about epoxy adhesives, and not specifically about Araldite 2015-1. So, results regarding the ageing of an epoxy adhesive might have varying degrees of applicability for the adhesive in this report. Anyway, they also include some testing in regular non salinated water. The results in regular water does not differ significantly from those in saltwater and both results agree with the manufacturers tests in that there is not any great effect on the bond strength. The article does however explain that there are processes taking place that affect the adhesive, but they counteract each other. The two processes are physical ageing and a reduction of the glass transition temperature (Tg) of the adhesive. The reduction of the Tg happens when the polymer absorbs water and it reduces the tensile strength of the adhesive, but increases the strain before failure. Physical ageing on the other hand is the slow relaxation of polymer chains into thermodynamic equilibrium. This causes their tensile strength to increase, but their strain before failure to decrease. So, because of the complementing nature of these processes, there is no noticeable change in the mechanical properties of the adhesive, and in some of the ageing tests they even increased. However, the article does mention that it is not uncommon for the properties of a polymer or adhesive to improve during aging before they start to deteriorate. Additionally the tests in the article, were only performed for 90 days, which is much shorter than the foreseeable lifespan of the adhesive joint. [24][25][26][27]

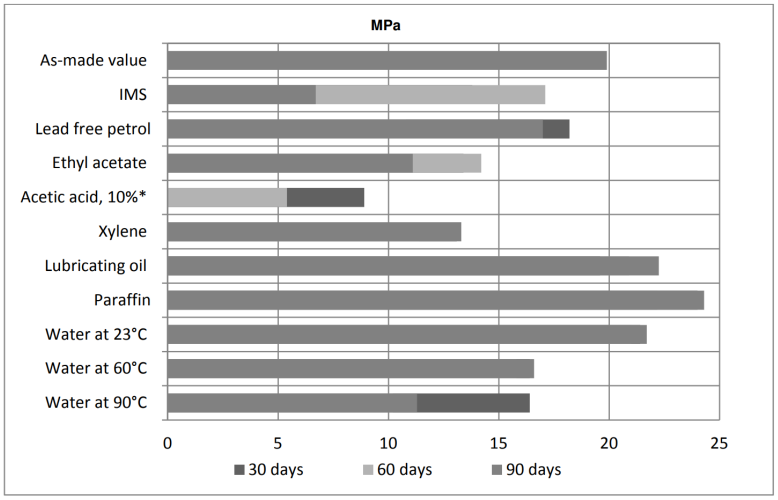

Fig. 5: Lap shear strength of Araldite 2015-1 versus immersion in various media (ISO4587) (typical average values). Tested on sandblasted aluminium after being cured at 40 °C for 16 hours and tested at 23 °C.*The adhesive degraded in the acetic acid after 90 days.[24]

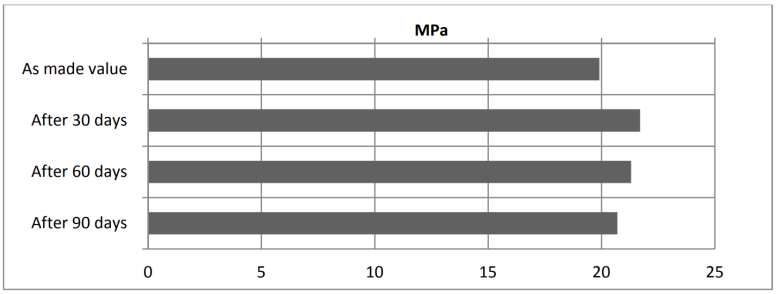

Fig. 6: Lap shear strength of Araldite 2015-1 versus tropical weathering (ISO4587) (typical average values). Tested on sandblasted aluminium after being cured at 40 °C for 16 hours and tested at 23 °C. Tropical weathering means exposure to a relative humidity of 92% and 40°C.[24]

The conclusion regarding aging is that since there have already been a lot of tests done in the area no further investigation will be done in this project. Since, to go beyond what has already been done, the aging tests would have to be done for a longer time than 90 days or simulate this extra time by employing harsher conditions. However, there is not enough time in this project to conduct tests that last longer than 90 days. Moreover, proper protocols to simulate the extra time is not known. Because, more general tools like the Arrhenius equation, might not be

enough to simulate harsher conditions since all aging process and mechanisms of the joints is not known.

2.2.4 Polymer incompatibility potentially causing matrix weakening

For this parameter two factors will be considered First, is if the adhesive is used to its full potential. If not, then it could be changed to an adhesive with worse general performance but equal performance in this specific case. This would be done in an effort to lower price, or to get an adhesive that is easier handle or to gain some other benefit. The other thing to consider is a hypothesis that the current adhesive might weaken the underlying CFRP laminate, which could then warrant a change. A strength loss due to weakening of the matrix is especially unwanted since it might compromise the underlying composite, making it harder to predict the strength of the joint. It is also worth mentioning that this parameter or the question if the adhesive should be changed is especially important because it affects other parameters such as aging and strain rate. So if the adhesive is changed, potential aging and strain rate tests done on the old adhesive will be of little value when characterizing the strength of the adhesive joint. This is because aging and strain rate are parameters that are closely related to the specific adhesive that is used. Aging and strain rate are furthermore parameters that require a lot of time and tests to determine. Additionally, as discussed in section 2.3.1, adhesive strength in an adhesive joint is very much a system parameter. This means, that new adhesives should be tested with the same ”realistic” tests that have been used to evaluate the current adhesive.

Now to address the potential matrix weakening effect of the current adhesive. Why this situation is handled separately from general strength might not be immediately apparent. Because potential matrix weakening could just be regarded as another factor in the complex system that decides the strength of the joint. So, the reason why this factor is handled separately is because damage to the underlying composite skin layer is especially unwanted. But it is also handled separately since both the underlying composite and the patch use a vinyl ester matrix unlike the adhesive which is epoxy based. Looking at the theories of adhesion, this difference in the polymer used for the matrix and the adhesive might affect the bonded joint in many different ways. Effects that depend on the chemical similarity of the adherents is for example the chemical effect and the diffusion effect. However, epoxy and vinyl esters are not singular polymers but groups of polymers and both can be made in many different ways, with different backbones and different epoxy groups. A more thorough explanation of the chemistry of epoxies and vinyl esters will be avoided because that would stray too much from the focus of this report. Instead a short walkthrough of the differences and similarities of vinyl esters and epoxy

resins will be given. [28] [29]

Thus, the short explanation is that both chemicals can be created from the same type of backbone such as the common bisphenol A diglycidyl ether (BADGE) molecule. The BADGE chemical is in itself the most common epoxy resin and has a bisphenol A (BPA) backbone and one epoxide group at each end of the molecule (see figure 7 for more details). More BPA can be added to the BADGE molecule to create a longer backbone consisting of more BPA units but with the same epoxide end groups. However, when vinyl ester is created from the BADGE chemical the BADGE molecule reacts with a carboxylic acid such as acrylic acid. The acrylic acid will then inhabit the end positions and the BADGE molecule will become the backbone (see fig 7 for more details). Similarly as with the epoxy resin more BPA can be added to the vinyl ester to create a longer backbone while retaining the same end groups. With short backbones there will be a higher concentration of end groups, but with long backbones the effects of the end groups on the overall behavior of the molecule will be less noticeable. Thus, in the case when a vinyl ester and an epoxy have the same backbone that also happens to be quite long their chemistry can be assumed to be rather similar. [28] [29]

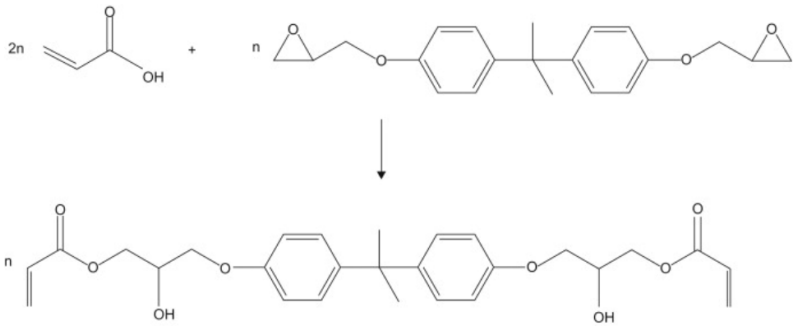

Fig. 7: The synthetisation of a vinyl ester resin from a bisphenol A diglycidyl ether molecule (BADGE) and acrylic acid. The BADGE molecule visible in the top right corner of the figure has a bisphenol A (BPA) backbone and epoxide end groups. Visible at the bottom of the figure, the vinyl ester resin created after the chemical reaction has a backbone of BPA and vinylic groups as well as ester linkages at the ends of the molecule.[29]

Moving back to the original problem, which is a potential chemical mismatch between the vinyl ester resins of the sandwich panel and glass fiber patch with the epoxy based adhesive. Even without specific information regarding the reactivity of the matrix and the adhesive, a more general discussion can still be useful. For instance fig 11 showing the shear lap strength of the Araldite 2015-1 makes it

clear that different polymers or composites with different polymer matrices can have very large differences in their adhesive bond strength. However, the exact reason for these differences is not clear. After an initial search no literature has been found that either confirms or denies the weakening of vinyl ester matrices when in contact with epoxy adhesives. This could indicate that matrix weakening is not a problem or on the other end of the spectrum that further research is needed on this specific topic.

Potential support of the matrix weakening is however acquired by looking at some basic pull tests. In these tests the fiberglass patch has been glued to the carbon fiber sandwich panel which in turn is attached behind a circular fixture. All of this can more clearly be seen in figure 8a. Several 90 and 45 degree pull tests have been performed and some notes are provided regarding the nature of the failure in the tests. In the 90 degree tests the patch comes loose with no adhesive left on the sandwich panel and a little of the carbon fiber attached to the adhesive on the patch. In the 45 degree tests however there has been significant delamination of what seems to be the uppermost carbon fiber layer as can be seen in figure 8b and the adhesive joints fail at lower loads. Nonetheless, the delamination in the 45 degree tests is mostly likely caused by the steel insert starting to turn over and this could also account for the lower loads at failure. The different manner in how the samples fail makes it hard to compare them. Nevertheless, in both tests the load on the patch does not exceed the listed tensile or shear stress of the adhesive, potentially supporting matrix weakening.

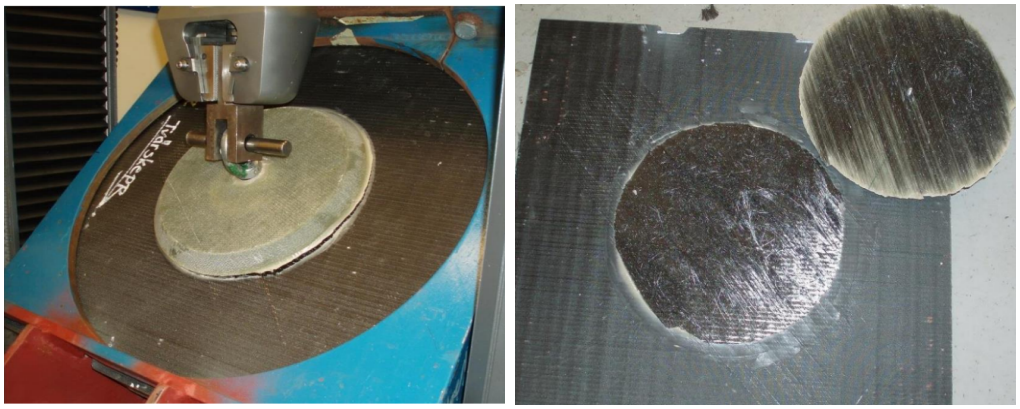

(a) (b)

Fig. 8: (a) The test setup used to see how much load the adhesively attached patch can withstand before failing. The blue square with a circular hole is the steel fixture that holds the black carbon fiber sandwich panel in place and the grey circle on top is the glass fiber patch which is attached to the tensile testing machine. (b) Adhesively attached patch pulled apart from a carbon fiber sandwich panel. This is how a test sample from (a) might look after testing. The prevalence of carbon fibers on the patch suggests an adherent failure and delamination of the carbon fiber laminate.

2.2.5 Connecting matrix weakening to theory and pull tests

Firstly the much lower than expected strength of the joint might indicate that the epoxy adhesive is a bad match for the vinyl ester resin of the sandwich composite sheets. One adhesive theory that is especially pointed out to have an effect on polymers is diffusion bonding. Polymers are generally immiscible unless very similar due to the large size of polymer molecules giving little entropic driving force for mixing. This could explain the low bond strength in this joint, but as mentioned before, the epoxy and vinyl ester could be quite chemically similar depending on the specific epoxy or vinyl ester used. Diffusion bonding is also not the only relevant bonding theory that can be applied and the matter of stress concentration that will be brought up in section 2.3.1 could also be relevant in this case.[30]

However, to get a better understanding of the failure of adhesives joints, more background information is needed. Firstly the principal ways in which an adhesive joint can fail will be presented. The modes of failure in an adhesive joint are adherent failure, cohesive failure and adhesive failure and they can be seen in figure 9. Adherent failure is when the pieces that are to be adhesively bonded break in some way like the delamination seen in the 45 degree tests. Cohesive failure is when the adhesive itself fails, which can be noticed by observing that there is adhesive

on both of the pieces that have been pulled apart. The final failure mode, adhesive failure is when the adhesive fails to stick to one of the pieces that are to be joined together. This failure can be recognized by only finding adhesive on one of the pieces that have been pulled apart. Among these failure modes, adhesive failure is generally unwanted because it suggests that the adhesive doesn't stick well to the adherents. However, adhesive failure can also be caused by insufficient surface preparation of the adherents or by having a too thin layer of adhesive. Nevertheless, this mode of failure means that neither the full strength of the adhesive nor of the adherents are used which is a waste of potential. [31] [23]

Fig. 9: The three principal modes of adhesive joint failure visualized.[31]

Both cohesive and adherent failure are said to be wanted because then the joint has utilized the full strength of either adhesive or adherent. In the case with the patch, it could be argued that an adherent failure is most wanted if the strongest possible joint is wanted. Since, if there is a cohesive failure, the adhesive could be improved until there is an adherent failure. To change the adherents would be harder because the adherent that isn't the patch is probably part of an already existing structure on a ship, plane or radio mast for example. Nonetheless, an adherent failure could also be unwanted because of damage to the underlying structure that would need to be repaired. In that case it might be worth it to sacrifice some joint strength. However, care should be taken when striving to achieve a cohesive failure because it can also be caused by having a too thick adhesive layer and the adhesive strength is not fully utilized. This is explained further in section 2.3.3. The adhesive joint failure of the 45 degree test is hard to evaluate due to the overturning of the steel insert. Although, the 90 degree test can still be analysed and here the joint fails in a mostly adhesive manner, but there are also signs of adherent failure. This result is rather good if an adherent failure is wanted. The results could however indicate that slight improvements could be made in pretreatment of adherents or perhaps small adjustments in the adhesive thickness. [32][31][32]

Continuing, to better understand adherent failure and delamination fracture mechanics should be investigated. According to fracture mechanics, failure can occur in three main ways, referred to as mode 1 opening, mode 2 sliding shear and mode 3 tearing, these modes are illustrated in figure 10. In the case of laminated materials such as the CFRP used in the skins of the sandwich panel, all these failure

modes are very likely to cause delamination. However, less energy is required for laminated composites to fail via mode 1 than through mode 2 and it is uncommon for them to fail due to mode 3 in a pull test. With the above information information it could be interesting to perform new 45 degree tests where the steel insert doesn't start to overturn and compare them with the 90 degree tests. Moreover, it is also not unexpected to see some delamination in the 90 degree pull test since this way of loading would cause mode 1 delamination which requires the least amount of energy. [31]

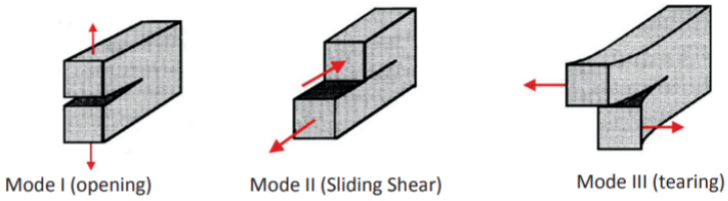

Fig. 10: Three main modes of failure in a material when it fractures because of a propagating crack.[31]

Now to summarize this rather lengthy discussion about changing the adhesive. First, If the adhesive is changed results from more complex parameters such as strain rate and aging will be of little use, thus the decision of changing adhesive should be taken early, or parallel studies of the old and new adhesive should be conducted to save time. Second, when comparing the new and old adhesive in a simple test one must be aware of the many limitations in standard industry tests. Third, potential matrix weakening due to incompatibility between adhesive and matrix is not ruled out, but stress concentrations could explain the results from the reviewed pull tests.

2.3 Mechanical testing

Here theory related to mechanical testing is presented to motivate the potential importance of some parameters that are related to mechanical testing. This section will also motivate the types of mechanical tests and properties that are the most important.

2.3.1 Mechanical testing methods

To properly model something with FE methods, knowledge about the object is required in order to mimic it. A lot of information about the mechanical properties of the adhesive is available and can be seen in table 1. Additionally, material data for the CFRP and GFRP that is used in the sandwich panel is also available and data about the foam core of the sandwich panel is provided by the manufacturer. However, this is still not enough. When using FE modeling it is impossible to perfectly mimic physical tests and therefore one should always strive to compare the FE test results to physical tests. If results from physical tests performed by others are deemed to be insufficient for use in comparison with the FE modeling then further physical tests should be conducted. However, there are a multitude of mechanical tests that can be done, but there are not enough resources to do them all. Literature on the subject will be reviewed to decide which mechanical test to conduct.[33]

Table 1: List of some tensile and flexural properties for Araldite 2015-1. The adhesive cured at 40 °C for 16 hours and tested at 23 °C. The tensile testing was done according to ISO 527 and the flexural testing was done according to ISO 178, both tests shows typical average values.[24]

Tensile strength	31 MPa
Tensile modulus	1600 MPa
Elongation at break	4.2%
Flexural strength	43 MPa
Flexural Modulus	1800 MPa

Tensile testing is one of the most common mechanical tests will be handled first. In a tensile test, a sample is pulled by the testing machine until it breaks. Properties such as yield stress, ultimate tensile stress, ultimate strain and tensile modulus can be measured to name a few. Parameters that can be varied during testing include temperature, strain rate and testing protocols. In composites, because of their anisotropy, the direction is also a parameter that can be varied.[33]

Another mechanical test is the flexural test. It is done by having a beam of the material resting on two supports and then a one or two pronged indenter is pushed

into the beam. If one pronge is used it is called three point bending test, and with two prongs it is called four point bending test. This pushing will bend the beam causing compressive stresses on the side that is pushed by the machine and tensile stress on the opposite side. Properties that are determined by flexural tests are flexural stress, flexural modulus and deflection. The test parameters that are often varied is the distance between the supports, specimen size, one or two pronged indenter and at what deflection to stop the test.[33]

Compression testing is done to evaluate a material's resistance to crushing loads. With compression testing compressive yield stress, compressive ultimate stress, compressive strain and compressive modulus can be determined. Compressive testing is usually done with one of three methods, end loading, shear loading or a combination.[33]

A test that is fundamentally different from the previously mentioned is strain rate testing, because it is a dynamic test. Materials can behave very differently when loaded at higher speeds, for example the yield stress can be doubled compared to its static value. Static testing or more accurately quasi static testing is done at strain rates of 10^{-5} to 5/s and if strain rates above that are used then the test is considered dynamic. Strain rate testing can in theory be applied to the previously mentioned mechanical tests. Nevertheless, with increasing strain rate more specialized test methods are required which limits how the tests can be conducted. At low dynamic speeds (around 10^{1}/s) drop high velocity hydraulic machines can be used and at very high strain rates (around 10^{6}/s) a plate impact machine can be used. [34]

To determine the shear strength is important when it comes to adhesives, because they are often subjected to these kinds of loads. A very common mechanical test used for testing the shear strength is the shear lap strength test. A shear lap strength test is conducted by adhesively attaching two rectangular bars to each other with a small overlap and the bars are then pulled apart in such a way that the adhesive is stressed in a shearing manner. The maximum force during testing is measured and then divided with the overlap area to get the shear lap strength of the adhesive. Figure 13 below can serve to further help the reader understand how the test is set up. This type of test has been done on a number of different materials joined with the Araldite 2015-1 adhesive and the results of these tests are presented in figure 11 and 12. [32]

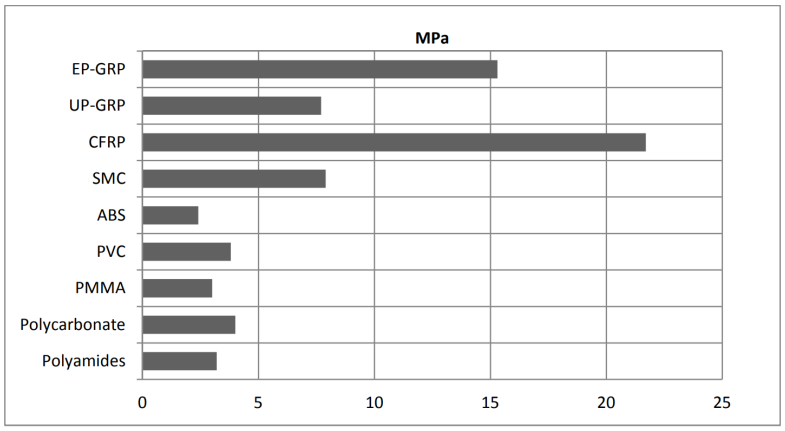

Fig. 11: Average lap shear strengths of typical plastic-to-plastic joints tested according to ISO 4587. The adhesive was cured at 40 °C for 16 hours and tested at 23 °C, the plastic surfaces were lightly abraded and alcohol degreased.[24]

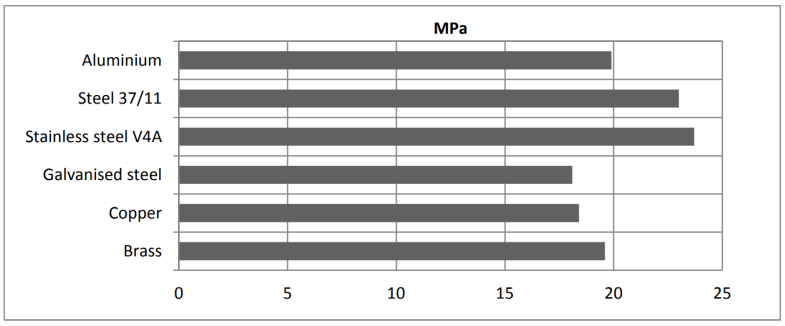

Fig. 12: Average lap shear strengths of typical metal-to-metal joints tested according to ISO 4587. The adhesive was cured at 40 °C for 16 hours and tested at 23 °C, the metal surfaces were sandblasted.[24]

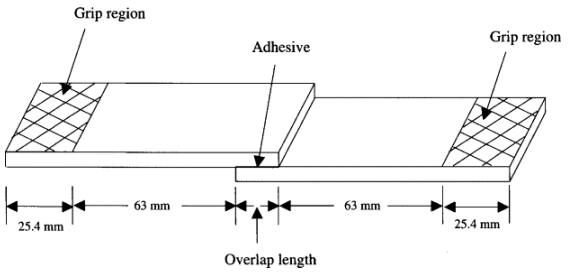

Fig. 13: Figure shows the setup of a shear lap strength test.[22]

Although standardized and simple to conduct, the shear lap strength test can be quite misleading for a number of reasons. Firstly, specimens tested in this way often fail because of tensile stress rather than shear stress. This happens because the bars used during testing are relatively thin in relation to their length and thus they are bent and warped during testing which causes compressive stress concentration in the middle of the overlap area and tensile stress concentrations at the edges. The tensile stress at the edges is often much higher than the global shear stress calculated from the shear lap strength test and is therefore many times the real cause of failure in the joint. This fact also highlights that even though adhesives have a more uniform stress distribution than bolts and other mechanical fasteners, as mentioned in section 2.2, great stress concentrations can still arise in adhesive joints. Secondly, test results from a particular shear lap test are not easily compared with other types of joints or even with shear lap tests where some of the testing parameters have changed. For example, intuitively since the shear lap strength is given in MPa, one might assume that doubling the area doubles the strength of the joint and this is perhaps almost the case if the overlap area is doubled by doubling the width. Is the length of the overlap area doubled however, there might not even be a 30% increase in strength. [22][32]

What all of the above serve to highlight is that adhesive bond strength is very much a system parameter that is rather sensitive to the type of adhesive, type of adherent, type of joint and temperature. These complexities can also somewhat be deduced from figure 11 and 12 because of all the different materials that are tested and how greatly the shear strength varies especially for the different plastics. The difficulties brought up here with the shear lap strength test is not assumed to be completely unique for this method. Therefore, the mechanical test used to compare with the FE modeling results should preferably be from the same joint that will eventually be used. These results can of course not be found in general literature. Luckily, tensile tests with a setup that is meant to closely mimic the actual joint to be used has been conducted. The results from these tests will be highly suitable to use for both the FE modeling and the microscope analysis. Nevertheless, despite the difficulties in generalizing results from mechanical tests from other works, literature will still be reviewed regarding strain rate and adhesive thickness. These parameters will be reviewed because of their differences to static testing and for future work.

2.3.2 Strain rate of adhesives

Considering the application, the majority of loads experienced by the adhesive and the adhesive joint will be static in nature. Thus dynamic properties will be of less importance. Nevertheless, the adhesive joint will still be applied aboard a ship

that is supposed to handle rough seas and the military nature of the ship means that it could also encounter explosive shock. These two conditions definitely cause dynamic loading and things such as accidental bumps with heavy equipment or personnel in a hurry might also happen, so strain rate properties are still somewhat important. Lastly, as mentioned in the previous section, dynamic loading is fundamentally different than the quasistatic tests. Therefore, it might prove useful to look into this further. [9][35]

The adhesive is marketed as being resistant to dynamic loading. However, no articles examining Araldite 2015-1 adhesive were found, but articles that handle the strain rate of other epoxy adhesives were more abundant. In general, epoxy adhesives and also other types of polymeric adhesives are sensitive to strain rate. The general trend is that strength and stiffness increase, while ductility decreases with increasing strain rate. But, there are many factors that complicate this picture. When researchers tested a polyurethane adhesive at low temperatures it exhibited a great strain rate sensitivity and failed at a much lower strain compared with static loading. However, when other researchers tested an epoxy adhesive at lower temperatures the epoxy was not as sensitive to strain rate as the polyurethane adhesive. Additionally, at the same low temperature but at higher strain rates the epoxy adhesive even required higher levels of strain before failure than it requires at room temperature during static loading. There are also large differences between the high strain rate compressive and tensile behavior at higher strain rates for polymers. The difference between adhesives can even be seen at static loading when comparing Araldite 2015-1 and Araldite 2014-2. Both adhesives are epoxies and are made by the same manufacturer, but they still have quite differing properties. [36] [35] [37]

After establishing that the general trends are not all encompassing and that there exists large differences between adhesives, some results from an examined article will be presented. The article have two dimensions to their tests both temperature and strain rate. The temperatures examined was 23 °C, -20 °C and -40 °C and when tested statically (at a strain rate of 10^{-4}/s) the strength and stiffness increased more and more with lower temperature just as the strain at failure and fracture energy decreased more and more. When different strain rates (10^{-4}, 1000 and 2000/s) were tested at 23°C the trend was not as clear. When strain rate increased to 1000/s the adhesive became stronger and stiffer and the strain to failure as well as fracture energy decreased, but not as much as it did at -20°C. Then at the strain rate of 2000/s the strength and stiffness continued to increase and the strain to failure also decreased, but the fracture energy had actually increased compared with the 1000/s test but it was still lower than the 10^{-4}/s test. [36]

Another interesting experimental result comes from varying the strain rates at

lower temperatures. At -20°C all the previously mentioned properties of the adhesive increased as the strain rate increased, except for the stiffness which decreased with increasing strain rate. Then at -40°C the results were quite different with a smaller increase in maximum load and now the stiffness did again increase as the strain rate increased and the strain at failure decreased gradually with the strain rate. The fracture energy however, first increased at 1000/s, but then decreased to a lower value than the 10^{-4}/s strain rate. [36]

These test results highlight the quite complex behavior of strain rate and its temperature dependence. However, it can be somewhat explained by a phenomenon known as strain softening. Both low temperature and high strain rates generally make adhesives stronger, stiffer and less ductile. Strain softening however, counteracts this behavior and is caused when high strain rates transform mechanical energy to heat which locally raises the temperature in the tested adhesive. Thus, the explanation of the results from the above experiments is that temperature, strain hardening and strain softening interact and at different temperatures and strain rates some of the effects are more or less dominating. In conclusion, strain rate is definitely an interesting parameter for this project, but is not as interesting as the static properties and is much harder to experimentally test or to model theoretically. Because of that, this report will not investigate the effects of strain rate on the adhesive any further. [36][7]

2.3.3 Adhesive thickness

Moving on, a parameter that might seem rather simple at first, but in reality requires more thought and consideration is the adhesive thickness. With adhesive thickness just like aging there are already some guidelines provided. The guidelines state that the thickness of the applied adhesive layer should be 0.05-0.1 mm. Nonetheless, many of the standard industry tests can be misleading and it is specifically mentioned that data from datasheet is not guaranteed unless specifically stated to be. So literature on the subject of adhesive thickness was investigated to see if there were any general trends. In the examined article they begin to discuss the limitations of analytically determining the optimum thickness. Because according to the authors, theory on the subject suggests that the adhesive layer should be as thick as possible to get optimal strength from the joint, but in reality this is not the case. Instead, according to experimental results the thickness of the adhesive needed to get optimum strength is dependent on what type of joint that is used, highlighting that the joint used for testing should be similar to the final joint used. In shear lap joints and in joints subjected to peeling some form of optimum thickness is observed. Butt joints however, which can be seen in figures 14 and 15 should have as thin of an adhesive layer as possible and practical while

still maintaining full coverage of the joint and a good interface. [24][32]

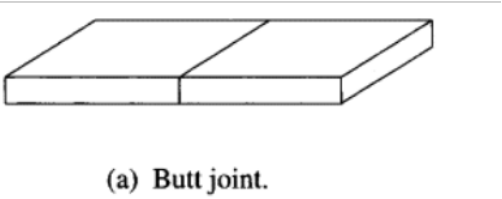

Fig. 14: Illustration of a simple butt joint.[22]

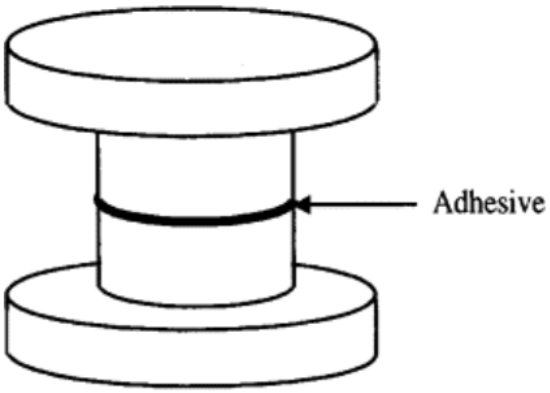

Fig. 15: Another example of how a butt joint might look, this specific configuration is well suited to be used in a tensile testing machine.[22]

Clearly this means that the as thick as possible guideline from old theory and experiments do not agree and the authors present two reasons for why experiments disagree with theory. The first reason is that a larger adhesive thickness would increase stress concentrations by providing a longer lever arm for the forces to act on. The other reason is imperfections in the adhesive joint such as air bubbles and voids which are more likely to form as the thickness increases. These two problems are the reasons why thicker layers of adhesive might cause cohesive failure (as mentioned in section 2.2.5). Because of the incoherence of old theory and experiments, the authors try to modify theory with some experimental results and achieve a pretty good fit between their new model and experimental results. With their model, they predicted an optimum thickness of 0.16 mm for one adhesive which according to their experiments should be around 0.11 mm. The other adhesive they analyzed had a predicted optimum of 0.1 mm, but the testing did not indicate an optimum or at least something closer to 0.2 mm. The prediction for the latter of the adhesives was still somewhat in line with the manufacturer's

guideline of 0.05 mm to 0.1 mm, which is good in a sense. But at the same time there is still a deviation especially compared with the experimental results which might also show that the manufacturer's guidelines shouldn't be blindly trusted. [32]

Thus, the results from this article does not yield a perfectly usable analytical formula, but they reference a source stating a general optimum thickness of 0.05-0.15 mm. Moreover none of the many other articles they reference indicate that there would be a benefit of increasing the adhesive thickness past 0.5 mm. Thus, with the results from this article and with the general guidelines from Araldite further investigations seem unnecessary in the scope of this project considering the limited timeframe. What can be done however is to make sure that test samples that are created follow the guidelines from this article and from the manufacturer. [32]

2.4 Microscopy techniques

There are two main types of microscopes, optical microscopes and electron microscopes. An optical microscope is a device that uses visible light and a series of lenses to magnify images. The electron microscope instead uses electrons as an illumination source and focuses them with the help of magnetic lenses. Electron microscopes can provide far higher resolution than an optical microscope, but that resolving power comes with its drawbacks. The two basic types of electron microscopes are transmission electron microscope (TEM) and scanning electron microscope (SEM). Both these microscopes limit the types of samples that can be examined. TEM requires that the emitted electrons can pass through the sample limiting its thickness to about 100 nm. SEM on the other hand requires an electrically conductive sample to avoid charge buildup. Additionally, both types of microscopes require the sample to be placed in various degrees of vacuum. These vacuum chambers are often limited in size meaning that the examined samples need to be small. So because of the limitations on sample size and since the extra resolution is deemed unnecessary, optical microscopy will instead be used in this thesis project. [38] [39]

The optical microscope is an old tool and during its many years of service many variants have been made, ranging from basic ones to very advanced designs. These advanced designs include phase contrast microscopy and confocal microscopy. Another advanced microscope that has been recently developed and that can replace the regular stereo microscope is the digital microscope. It is purpose built to transfer the image to the sensor of a digital camera and view it on a monitor, thus lacking any means to view the image with the naked eye. The lens of the digital microscope and the sample stage can also be connected to electrical motors controlled with a computer. This increases the price of the microscope, but makes it very easy to use, requiring virtually no training. That is why a digital microscope has been chosen to be used in this master thesis work. To further improve image quality polarized light will also be used to enhance contrast and the theory behind that will be briefly explained below. [40] [38] [41]

Light consists of an electric wave and a magnetic wave which are at a 90 degree angle to each other and both of them are perpendicular to the travel direction of light. If one considers a random ray of light it will consist of many different light waves and within a light wave the electric and magnetic waves will be at right angles, but between them the different electric and magnetic waves will be randomly oriented. Some crystaline materials such as doped poly(vinyl alcohol) will absorb all light that has its electric wave completely out of phase with its crystal structure or in other words at a 90 degree angle to it. If the crystal is then rotated it will let more and more light through until almost all of it passes through

when it is aligned with the crystal structure.[40][42]

The interesting aspect here is that by placing a material such as doped poly(vinyl alcohol) right after the light source on the microscope, polarized light can be achieved, but when light is reflected on shiny surfaces it tends to change its polarization. Now by placing another polarizer somewhere between the returning light and the observing eye, it can be aligned to let light through that has the same polarization as the light that illuminates the sample. This will thus make it harder for much of the reflected light to reach the observer, thereby minimizing the effects of glare and getting a better contrast in the image.[40][42]

2.5 Finite element modeling

A potential method to use when developing the tools needed to evaluate the load bearing capability of the adhesive joint will be explored.

2.5.1 Basics of finite element modeling

FE modeling is the most widespread numerical analysis method that is used today. FE modeling was originally intended to be used in solid state mechanics to solve plate bending problems, but it proved much more versatile and has found use in all manner of different engineering and physics problems. The basic concept is to solve complex differential equations by approximating them with many simple differential equations. For example FE is widely used in crash test simulations for cars. If the car crash was to be described with a single differential equation with boundary conditions it would be hopelessly complex and equally difficult to solve. What is done in FE modeling is that the car is divided into many small parts called elements which are connected to each other with nodes. The elements can also be described by differential equations, but these equations are much simpler than the one that would have been used to describe the whole car crash. So because of their simplicity, these equations can be handled by a computer. Thus, the computer proceeds to numerically approximate answers for the differential equations of all the elements that make up the car and summarize them to get an approximation of the answer to the differential equation for the whole car. This is basically the whole FE process, somewhat simplified of course.[43]

To provide some more details behind the mathematics of FE modeling, it should be noted that the differential equations from the different elements are connected. Together all of these equations create a very large equation system which is what the computer approximates and solves. Additionally, since this is a mechanical analysis the equation system is solved by using Newton's second law F = ma. The discretization process is called meshing, so named because the object that is to be divided into smaller parts is done so with the use of a grid of intersecting lines known as the mesh. The intersection point between lines creates the edges of the elements and is most often the location of the nodes in the model (but some elements can have nodes in other places too). Nodes contain the positional information of elements in the form of X, Y and Z coordinates from a known coordinate system. Furthermore, the elements in the model also need to be assigned material properties. The material defines how hard it is to move (mass/density) and deform (stiffness) the model and it can be both linear, non linear or a combination of both. The material can also be either isotropic or anisotropic. In this thesis work the model that is used is going to be linear and it can thus be described by Hooke's law $F_x = Kx$ which for the whole equation system becomes equation 2

[43][44]

$$\bar{F} = K\bar{U}. \tag{2}$$

Where $\bar{F}$ is a vector containing all the forces that act on the model K is the stiffness matrix containing material stiffness properties and $\bar{U}$ is a vector containing the displacements of the nodes. However, to properly solve the equation system described by equation 2 the displacement of some elements need to be limited. This limitation could come in the form of the wall that the car is supposed to crash into which could be hindered from moving because it is of course attached to the floor. These limitations are called boundary conditions and it is the final piece of this basic FE description.[44]

Returning to the discretization, a denser mesh gives smaller elements and a more accurate solution. However, a larger number of elements means more differential equations to approximate and thus the time it takes to calculate the answer increases. Therefore, there is a rather fine balance between how accurate the answer needs to be and how long the calculation should take. There are of course many different techniques that can be utilized to reduce the calculation time and still maintain a fairly accurate answer. One way of doing this is to divide the model into several parts which can then be handled by different processor cores. This is an important feature especially if one has access to a computer or server with a large amount of cores. In most cases the dividing of the workload is done automatically, by the FE software.[43][44]

After considering the aim of this thesis project it has been decided to keep the FE model rather simple and therefore it will be based on a maximum stress criterion. That means that the maximum stress value in some key elements will be investigated, based on linear elastic theory, and compared with the strength of the material. Thus if the stress is above the strength of the material it will be considered to have fractured. Shipbuilding standards state that a safety factor of 3 should be used for structural parts made out of composites. This then places a somewhat lower demand on the accuracy of the ultimate strength prediction. The limited time of this thesis project also plays a part in choosing this FE technique, because the stress criterion is simple and easy to implement and does not require proficiency in FE modeling, nor does it require particularly complex material data. However, to improve the accuracy without making the FE modeling harder an interacting stress criteria will be used. This criteria takes the quadratic sum of strength ratios, the ratio between actual stress in the element with the ultimate strength of the material, deemed relevant for the fracture of the sample and adds these together. If the sum is equal to 1 or more a fracture occurs. As the

work has progressed it has become more apparent that it probably is the carbon fiber laminate that fails and since the fibers themselves are extremely strong the failure is believed to be matrix dominated. Therefore, the relevant stress for this type of failure will be the out of plane stress (Z), the XZ shear stress (XZ) and the radial tensile stress (RTS). How these are combined in the interactive stress criterion can be seen in equation 3 below, [45]

$$\left(\frac{\sigma_z}{\sigma_z^{max}}\right)^2 + \left(\frac{\sigma_{xz}}{\sigma_{xz}^{max}}\right)^2 + \left(\frac{\sigma_{rts}}{\sigma_{rts}^{max}}\right)^2 \geq 1 \Rightarrow \text{Material fracture.} \tag{3}$$

In equation 3 the variables σ_z, σ_{xz}, and σ_{rts} are the plane-, shear-, and radial-tensile- stress respectively. These are divided by the corresponding ultimate stress limits.

2.5.2 Modeling stress concentrations in the patch

Now, the final parameter that needs to be considered, is how the geometry such as size and shape of the patch itself and of the hull affects the strength of the joint. This was also believed to be one of the more interesting parameters, because an early theory regrading the adhesive joint was that the stiffness of the sample could be a major factor in determining the strength of the bonded joint. Additionally, there were also discussions to change the shape of the patch from the currently circular shape to a more oval shape to better handle angled loads. The reason for this is because in the conducted mechanical tests the load at failure was lower in the 45 degree pull test compared with the 90 degree pull test.

However, the ideas to change the shape of the patch was fairly quickly put on hold because the patch might be used for many different applications so to specialize it for a single load type now was not of interest. Moreover, the primary purpose is not to optimize load carrying but rather to define the load carrying ability of different patch sizes to help designers to choose the right patch. To introduce more patch shapes would distract from the main purpose.

Nevertheless, the stiffness of the patch and hull is still of much interest especially considering how the flexing of a joint introduces stress concentrations. As mentioned before, this could also explain the lower nominal stress at failure observed in previous tests. It was also noticed that when the thickness of the glass fiber patch, and thus stiffness, was increased, the load at failure was lower. This follows what other researchers have found. Namely that the stiffness of both the adherents should be matched. [22] [46]

The reason for this is stress shielding, because when one of the adherents is more

stiff, a high stress will be generated at small displacements, which can then cause the weakest link in the system to fail such as the adhesive or the carbon fiber skin. However, by matching the stiffness of the adherents larger displacements can be handled by the joint. Thus, if stress concentration and stiffness is a problem, this needs to be studied. Doing this by using manual calculations and experiments is tedious, time consuming and resource demanding. Therefore, FE methods might be an excellent way to reduce some of the manual testing. [22] [46] [32]

The conclusion from the discussion in this section is that geometry of the patch could be quite a complex parameter, which can also be realized by looking at all the possible joint types that exist. To reduce the complexity of this parameter, the geometries of the patch and hull will remain the same and instead the stiffness concentration will be studied since it seems to be a very general problem and an important factor in the failure of the joint. Moreover, the stress concentration is probably simple enough to be studied with FE methods, which is part of the goal of this master thesis project. Additionally, FE methods are very valuable tools if they can be used because of the time and resources they save. [32]

2.6 Summary of critical strength parameters

Now it is time to summarize all the discussions about the different parameters and whether they are to be focused on or not. As have been mentioned throughout this report, both time and resources are limited in this project, which means that even parameters that have been deemed to be of interest might not be investigated further.

When it comes to the compatibility between the adhesive and the adherents, it might very well be some chemical mismatch considering the results from figure 8b. This chemical mismatch is less likely to weaken the matrix of the carbon fiber laminate adherent. The results from mechanical tests can possibly be explained by the phenomenon of stress concentrations.

When it comes to aging and environmental resistance, rather thorough tests have already been done, and the one important test that had not been done was the effects of saltwater on the adhesive. Although a couple of sources were found on the subject, they indicated that the saltwater resistance of epoxy adhesives is good. The vinyl ester matrix also had a good chemical resistance in general and to saltwater in particular according to some articles. Thus, the only thing left to be done when it comes to aging and chemical resistance is to test speciality chemicals if there is need for that and to make very long aging tests that last well over 90 days in real time. So, this parameter is already well tested and it is outside the scope of this project to investigate it further.

The adhesive thickness parameter just like the environmental resistance parameter has been somewhat investigated before at least to the degree that guidelines can be provided on how thick the applied adhesive should be. This guideline has support in a couple of articles which state that a thin layer provides the best strength. Nonetheless, another article disagrees and suggest that a thicker adhesive layer be used. The problem with misleading industry tests also remains and the thickness of the adhesive is not so easy to change when considering the actual manufacturing of physical specimens. Thus, this parameter will be left out from this thesis project.

Strain rate is one of the more complex parameters and no data was found regarding the strain rate sensitivity of the adhesive. However, articles have indicated that most polymeric adhesives are strain rate sensitive, but that the exact nature of this strain rate sensitivity can vary widely. Despite this, strain rate will not be investigated further because its complex nature makes it hard to model with FE methods and also makes it hard to test experimentally.

Size, shape and other geometry related factors can be very time consuming to test if every aspect of it is to be examined. Additionally, this project aims to gain

a rather general understanding of the load carrying in the adhesive joint before moving to more specialized cases. Therefore focus will be on the stiffness of the joint and how this affects stress concentration in the joint via bending.

Possible future research on the different parameters that will not be covered in this report includes, the chemical mismatch of the adhesive and adherent and long time aging tests. Research can also be conducted on the optimization of the adhesive thickness, characterization of strain rate properties of the adhesive and testing of different patch shapes to optimize strength in specific directions.

However, the focus of this thesis project will be to model the adhesive joint with FE methods to understand what type of stress concentrations arise and to link these to the maximum load a joint can carry. The FE modeling will then be compared with previous mechanical tests to see if the predictions from the modeling are correct. Finally, the FE results will be complemented with microscope image analysis of samples that have already been mechanically tested.

3 Materials and Methods

Computer modeling, sample preparation for optical microscopy as well as the microscopic analysis itself have been conducted in parallel to efficiently use the limited time of this project. They are presented separately in this section for the convenience of the reader.

3.1 Materials and methods used for microscopic analysis

In the names of different carbon fiber fabrics the first letter is a type designation for fiber fabrics and the rest of the letters designates fiber orientation. The numbers denote weight in grams per square meter of fibers contained in the fabric. A BX fabric is made of two thinner plies where one ply has fibers oriented at a 45 degree angle and the other ply has its fibers oriented at a -45 degree angle. In a UL fabric there is only one thick ply with all fibers in the same direction. The BLT fabric just like the BX fabric is made of two thinner plies, but in this case one of the plies has its fibers in a 90 degree angle to the other ply. The QXLT fabric has quasi isotropic properties in the plane directions and is equivalent to a BX fabric stacked on top of a BLT fabric.

The number in the core name designates its density in kg/m^3 and with increasing density the mechanical properties of the core is also improved. All the carbon fiber fabrics used are non crimp fabrics stitched together with a polyester thread. The fiber used in the carbon fiber plies is Toray T700S, and the glass fibers in the patch is E glass. The resin used to manufacture a laminate from the different carbon and glass fiber plies is a vinyl ester from Reichhold with the designation Dion 9102. Critical material data for these materials can be seen in table 2.

The specific microscope used during examination of the samples is a VHX-6000 control box with a VHX-S650E free angle observation system and a VH-Z100UT lens. The setup can be seen in figure 16. The VH-Z100UT is a universal zoom lens with a magnification between 100-1000 times, but due to lens distortion it is best to stay between 200-900 times magnification. For all the microscope images in the report the stitching function of the microscope has been used. This function scans through the sample in the X, Y and Z directions taking multiple images and then stitches them together. This function saves time and allows for inexperienced microscope users to achieve good image quality. To improve image quality polarized light will be used to enhance contrast.

Table 2: Data for some of the materials used in the examined sample.*For the PVC core shear strain at failure is listed. [47][48][49][50]

-	Density [Kg/m^3]	$TS[MPa]$	E_x $[GPa]$	Strain at failure [%]
PVC foam core	80-130	2.5-4.8	0.095-0.175	30-40*
Carbon fiber (T700s)	1800	4900	230	2.1
Glass fiber (E-glass)	2540	3400	72	4.7
Vinyl ester matrix	1050	80	3.17	5.2

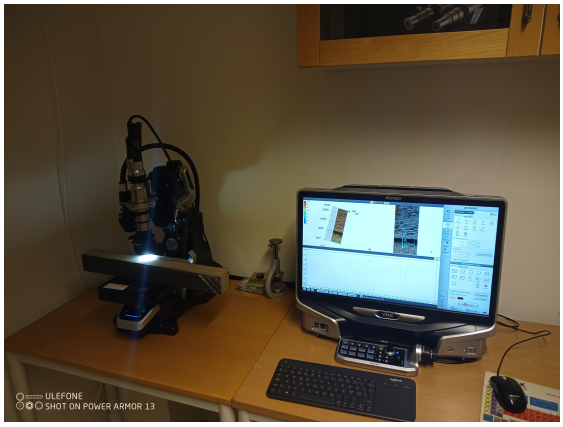

Fig. 16: The microscope next to the control box which is used to operate it.

Fig. 17: Two specimens can be seen in this image, they are the two sandwich panels stacked on top of each other along with their two large glass fiber patches. These pieces were separated during tensile testing of the patches. The specimen that was used for the microscopic analysis in this report is the bottom sandwich panel and the patch with the number 55717 (the fracture load). At the top of the image is the test sample, from figure 1a and 1b, that was used in the microscopic evaluation.

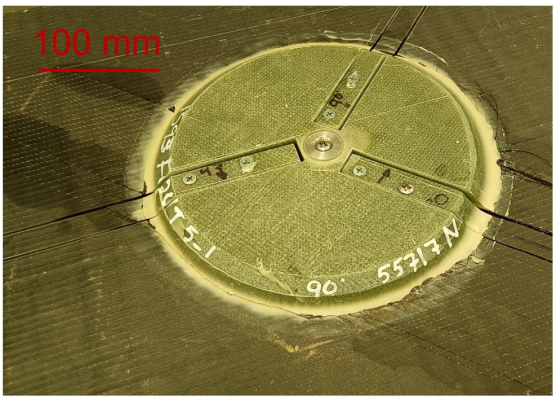

Fig. 18: Glass fiber patch specimen from which the samples are taken for the microscopic analysis. The samples were cut in 0, 45 and 90 degree angles to the topmost carbon fibers, indicated by the numbers written on them.

Now, the specific samples examined in the microscope was a sandwich panel with a face that is 60 x 60 cm and a GRFP patch with a diameter of 25 cm. The GRFP patch consists of 19 QXLT850 fabrics with a total thickness of about 19 mm. The upper CFRP skin consists of three different types of carbon fiber fabrics, BX420, UL420 and BLT 420 in order from top to bottom and repeated once giving a total of six fabrics with a thickness of about 2.8 mm. The bottom CRFP skin has the same type of fabrics but is repeated 5 times giving a total of 18 fabrics and a thickness of about 8.4 mm. The core of the specimen is 6 cm thick and is made of H80 poly vinyl chloride foam from Diab. The adhesive is a layer of about 1mm Araldite 2015−1. The specimen can be viewed in figure 17 and 18 and for an explanation of the material designations see section 2.1.

The joint was tensile tested using an Instron 5984 universal testing machine, until failure using the rig shown in figure 8a. After failure, delamination of the CFRP could be observed, and a small amount of adhesive was left on the sandwich panel side of the joint. Thus, the fracture most closely resembles an adherent fracture. After testing, the sample was stored for at least several months partly in a warehouse with little climate control. This did however, probably not affect the specimen since all of its components have good chemical and environmental resistance.

After storage, the specimen was recovered and prepared for cutting with a water jet to make the samples that are examined in the microscope. The preparation consisted of drawing out guidelines for the waterjet cutter in a 0, 45 and 90 degree angle to the carbon fibers of the uppermost carbon fiber mat. After that, two screws per sample and one in the middle of the patch were used to reattach the glass fiber patch to the sandwich panel. These three samples are referred to as S0,

S45 and S90 in accordance with their angles to the topmost carbon fibers. The above procedures are illustrated by figure 18.

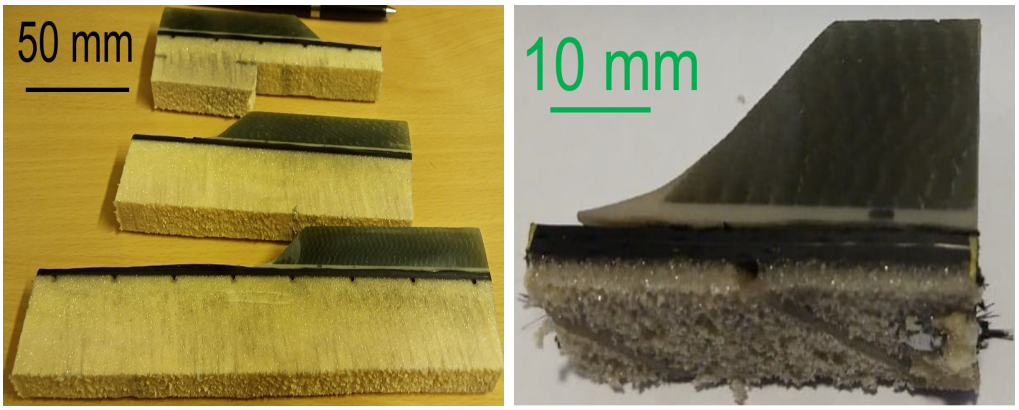

(a) (b)

Fig. 19: (a) One of the samples after cutting by water jet. (b) All the samples after removing most of the core, the lower carbon fiber laminate and reducing their length. Different samples have differing lengths depending on how far the delamination spread during cutting, because all of the delamination was to be examined in the microscope. (c) S0 sample after the last cutting.

After cutting the samples were examined in the microscope. Then they were further cut with a band saw removing half of the core and the lower carbon fiber laminate as well as making it shorter. The size of the sample after further cutting can be seen in figures 19a, 20a and 20b showing micrograhps of the sample before polishing. All the samples were then polished with sandpaper with grits of P120, P500, P800, P1200, P2000 and P4000. The S90 sample was hand polished while the S45 sample was machine polished during the rougher grits 120P, 500P and 800P and the S0 sample was machine polished when using the 200P and 500P grit sandpapers. The machine used for grinding was a Struers Rotopol-22, and polishing was done at 300 rpm with a constant water supply.

After polishing, representative parts of the samples were examined in the microscope to discover details that could reveal failure mechanisms and to pinpoint the starting point of the delamination. The polishing quality was deemed to be adequate, and some individual fibers could be distinguished. By combining visual features and relative measurements individual carbon fiber layers could be located. Some of these images are shown in figures 27 and 28 in the results section. The regions of interest in the physical samples which had been determined as critical

in the FE model were further cut out from the samples and polished. They could then be analyzed in the microscope with a higher magnification.

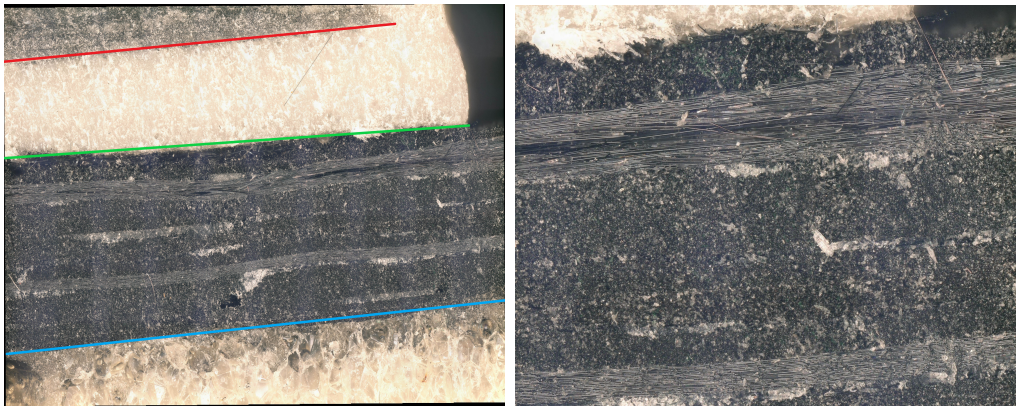

(a) (b)

Fig. 20: (a) Sample cut at a 90 degree angle to the topmost carbon fibers. This image is taken before polishing and shows the edge of glass fiber patch. The sample has 4 main parts, the glass fiber patch visible as a grey area above the red line. The adhesive visible as a whitish area between the red and green line. The carbon fiber laminate, which is the mostly black area between the green and blue lines. The PVC foam part of the sample is visible below the blue line as a white structure with many voids. (b) The image from (a) magnified on the carbon fiber laminate, some individual fibers that run parallel with the image can be seen.

This further cutting was done with a bandsaw to cut through the carbon fiber and the glass fiber, and the core was removed by cutting it with a regular box knife. After these procedures, almost all of the core was removed and the length of the sample was significantly reduced. During this cutting, the S0 sample was severely damaged. The S45 was also damaged, but most of the delaminated carbon fiber layers appeared intact to the naked eye. For the S90 sample, a metal hand saw was used to prevent damaging the delaminated carbon fiber layers. The appearance of processed samples can be seen in figure 19b.

After final cutting, the specimens were repolished to a higher quality, which would make it easier to distinguish the microscopic features of the samples. This further polishing was entirely done with the Rotopol- 22. The 120P, 500P and 800P grit sandpapers were used at a speed of 300 rpm, but for the 1200P, 2000P and 4000P grit sandpapers the speed was lowered to 150 rpm. After this the samples were again investigated with the optical microscope and these new images were used for analysis and comparison with the FE modeling results.

3.2 Materials and methods used in the FE analysis

The computer model of the patch was based on FE methods. The FEM model was generated using the Hyperworks 2021.2 program from Altair, solved with Ansys mechanical apdl 2021 R2 using a mechanical premium license from Ansys and the data were analysed in Altair's Hyperview version 2021.2 using corner data. To be able to utilize these sometimes demanding softwares, they will be run using a server. This server runs on Windows and has a work memory of 191 GB with a speed of 2666 MHz and a Intel(R) Xeon(R) Gold 6234 CPU with a clock frequency of 3.3 GHz and 16 threads.

In this thesis project, all the FE models are constructed in HyperWorks and based on a circular model with a diameter of 600 mm and a patch diameter of 70 mm and can be seen in figure 44 in the appendix. The circular model is only a quarter of a full circle, but is symmetrically loaded to mimic the tensile tests of the real physical samples to later enable comparisons. In this model, the carbon fiber laminate is 2.8 mm thick on both sides of the core and the core itself is 60 mm thick. The glass fiber patch is 19.2 mm thick and the adhesive is 1 mm thick. In the FE model the cards that determine how Ansys will solve the model are set, 5 components are present and represent the glasfiber patch, the stainless steel insert, the Araldite 2015-1 adhesive, the poly vinyl chloride core and the carbon fiber skins. Material models are assigned to the appropriate components and are based on data sheets from the manufacturers and can be viewed in table 3. To simplify modeling, all the materials was modeled as linear elastic.

Table 3: Material data for the 5 materials used in the FE models

-	Density [Kg/m^3]	E_x $[GPa]$	E_y $[GPa]$	E_z $[GPa]$	ν_x	ν_y	ν_z
Adhesive	1400	1.850	1.850	1.850	0.30	0.30	0.30
Core	80-130	0.095-0.175	0.095-0.175	0.095-0.175	0.40	0.40	0.40
Patch	1889	40.98	11.47	11.47	0.235	0.294	0.235
Skins	1444	116.7	8.18	8.18	0.285	0.294	0.285
Insert	8000	200	200	200	0.30	0.30	0.30

Two element types are used, solid 185 and solid shell 190. Solid 185 is used for the steel insert, the core and the adhesive. Solid 185 is also used for the glass fiber patch, but in this case key option 3 is set to 1 which turns this element into a layered structural solid to better mimic the properties of the glass fiber patch. For the carbon fiber laminate, solid shell 190 is used because it gives a more accurate shear stress response compared with solid 185 with key option 3 set to 1. The model was also meshed more densely in the area around the edge of the patch, and the elements here are about 2 mm in size instead of 10 mm millimeter, which is the size used for the rest of the model.

A coordinate system was established for the model, and this is important for the properties section of the model. The properties section provides further specifications to solid layered 185 and solid shell 190 and allows them to behave in more complex ways. More specifically, the properties are used to designate that each glass fiber or carbon fiber element consists of a number of layers with different properties. As has been explained in section 2 of this report, the properties of the different layers in glass fiber or carbon fiber are highly directional and thus the established coordinate system makes sure that the layer is placed in the correct direction.

Except for the base model with a 70 mm patch two other models were also created, one model with a 160 mm patch and one with a 250 mm patch.

The 250 mm model can be seen in figure 21 and 22 .Because of the similarities between the models the 250 mm will mostly be used from now on to represent the other models both in this section and in the results section.

These sizes were chosen because just as with the 70 mm model they are all included in a report where a number of different patch sizes and sandwich panels were tested to try to discover any patterns in the load bearing capability of the adhesive joint. The 160 mm model is identical to the 70 mm model except for the patch size, some small differences in meshing and the core which in this model is a H100 core instead of the H130 core of the 70 mm model. The carbon fiber laminate structure of the 160 mm model is also different, because it has one BX420, one UL420 and one BLT420 ply repeated once compared with the 70 mm model which has one BX610 ply and one BLT610 ply repeated once. The 250 mm model differs from the 70 mm model in the same way as the 160 mm does, but the core is a H80 core. Additionally, the 250 mm model has a much thicker bottom carbon fiber laminate, which consists of one BX420, one UL420 and one BLT420 ply repeated five times, which gives it a total thickness of 8.4 mm.

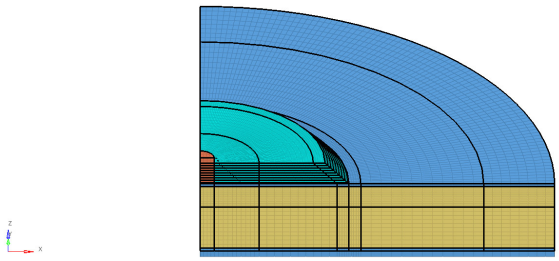

Fig. 21: Overview of the FE model, with a patch diameter of 250 mm. The blue components is carbon fiber laminate, red is the stainless steel insert, yellow is the PVC core and teal represents the glass fiber patch. Images with 70 and 160 mm patches can be viewed in the appendix.

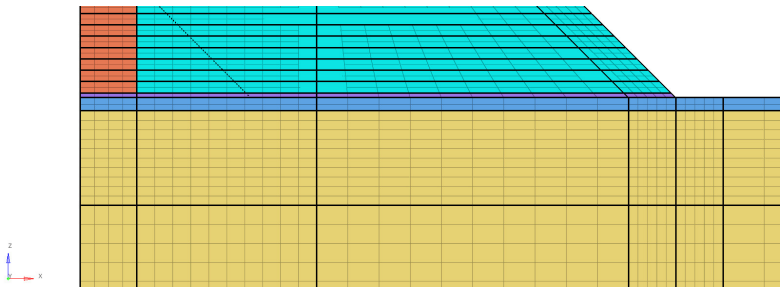

Fig. 22: Magnified image of the 250 mm FE model, the adhesive is visible as the purple colored component, and mesh lines used to divide the model into smaller parts are visible. The mesh line density is higher towards the the edge of the glass fiber patch, because stress concentrations and thus failure of the sample is believed to happen in the area close to the edge of the glass fiber patch. Therefore, it is important that the stresses in this area is resolved properly.

The 70 mm model is pulled with a load of 2608.5 N. That is a quarter of 10434 N, which is the same load used to fracture the physical sample. The load of 2608.5 N is further divided into 47 parts giving a load of 55.5 N, which is distributed evenly across all the nodes on top of the steel insert. The 160 mm model and the 250 mm model are loaded following the same principles but have a total load of 6575.1 N and 13929.3 N, because the physical samples they are based on required larger forces to fracture. The total load of these larger models are divided into 21 parts giving a nodal load of 313.1 N and 666.3 N. Furthermore, all the models have a boundary condition on top of the topmost carbon fiber element layer placed along a quarter circle that is 6 cm from the circumference of the model. This boundary condition simulates the steel fixture from figure 8a that keeps the physical samples

in place. Images of how the loading is applied and the applied boundary/symmetry conditions can be seen in fig 23 and 24.

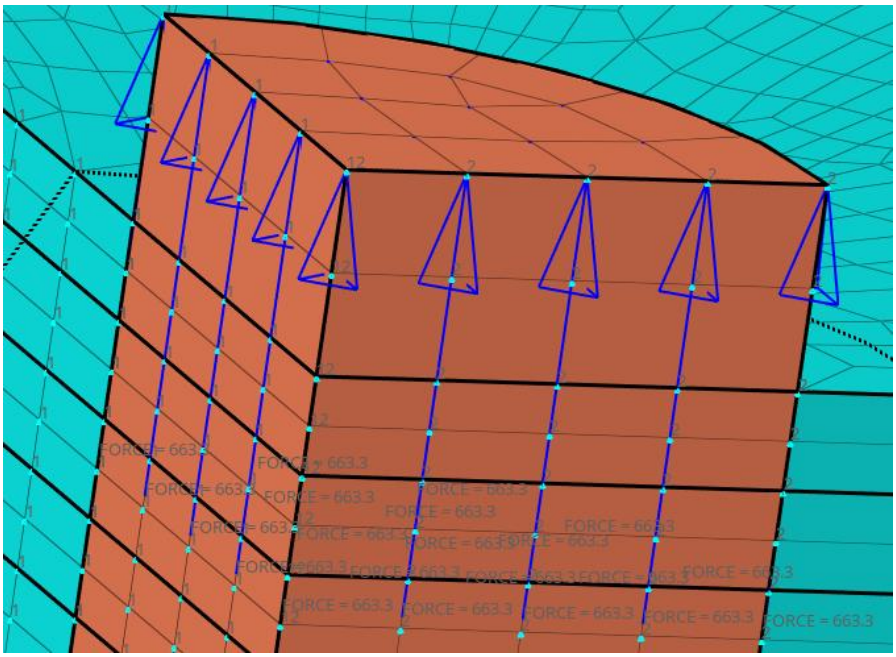

Fig. 23: Image showing how the 250 mm FE model was loaded. The loading force was divided among all the 21 nodes of the stainless steel insert (the red part of the image) and thus each node was loaded with a force of 663.3 N. The dark blue arrows indicate the direction of the loading force which is parallel with length of the steel insert and in the normal direction of the patch surface. In this image some of the boundary conditions applied to the model can also be seen. The boundary conditions are shown as small ones or twos along the surface nodes of the model. These boundary conditions prevent movement in the normal direction of the surface that they are applied to.

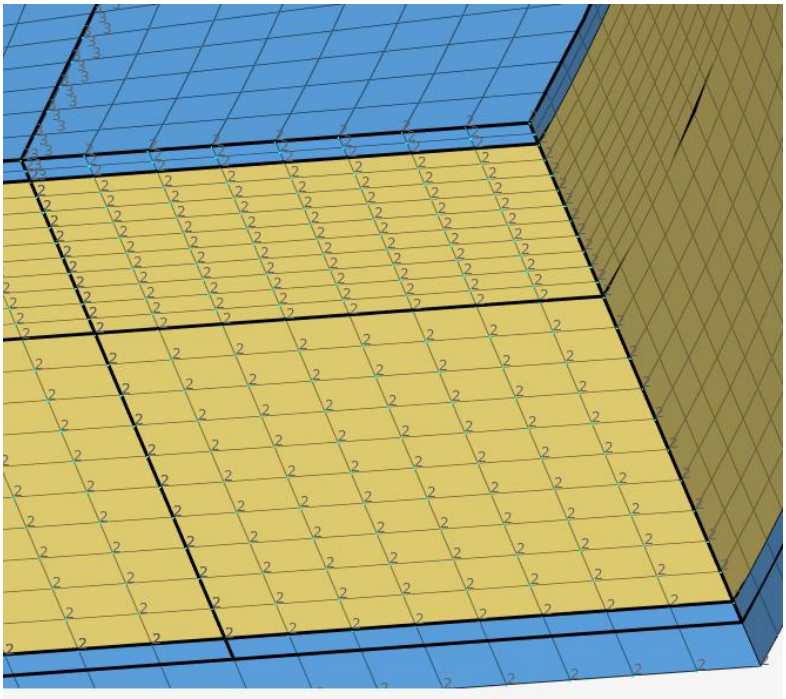

Fig. 24: Image showing more of the boundary conditions applied to the model. As in the previous image the boundary conditions are represented by small numbers in this case twos and threes. Moreover, just as before they prevent movement in the normal direction to the surface.

After finalizing, the three different models were exported to Ansys as a cdb file and solved. Then in Ansys, different stresses and strains were investigated in the model with focus on the edge of the glass fiber patch and the topmost carbon fiber layer directly beneath. Individual elements with the highest stresses and or strains were also examined to determine if failure had occurred. To get a proper analysis, three submodels were created one for each basic model. The sub models are the areas of interest from the regular models, but modeled in much greater detail, with more elements. In the submodels, every carbon fiber layer has its own element making the carbon fiber laminate 12 elements in the 250 and 160 mm submodels and 8 elements in the 70 mm submodel. Since every layer has its own element in the submodels there is no longer any need for the solid shell 190, and solid element 185 is instead used to model the carbon fiber laminate layer. The submodels are solved by first solving the regular models and then an Ansys subscript is used to gather the data from edge nodes in the interface between the regular models and the submodels and the subscript uses this data to solve the submodel.

With the submodels, a more detailed result was achieved, points of interest from

the different submodels were chosen. These points were 3 elements from each submodel, and these elements were the element with the highest out of plane stress (Z stress), the element with the highest RZ shear stress and the element with the highest radial tensile stress. The 250 mm submodel can be seen in figure 25 and 26, while the image showing the points of interest can be seen in figure 35 in the results section. These points can be viewed more in detail in figure 35 in the results section.

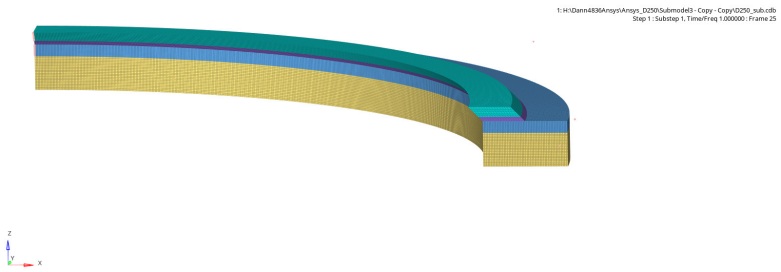

Fig. 25: The submodel of the 250 mm model. There are 3 submodels, one for each patch size, but since they are very similar in appearance only the 250 mm image is shown. The submodel is the area of interest from the regular model that has been extracted and modeled with a much higher mesh density.

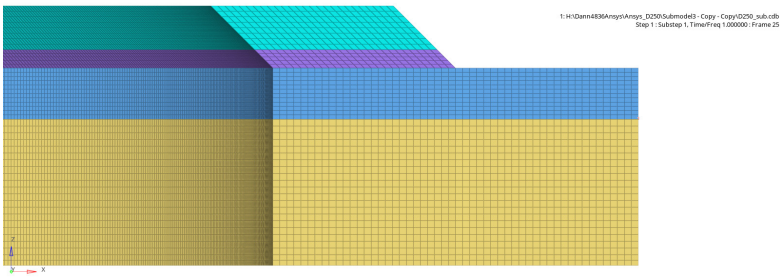

Fig. 26: Magnified image of the submodel showing the mesh lines in more detail. Every carbon fiber layer has its own element compared with the regular model where one element represents 6 layers. Thus, in this submodel the carbon fiber laminate is 12 elements thick instead of 2 giving a better resolution of the stress levels, but at a cost of higher calculation times.

4 Results

4.1 Optical microscopy

In this section images of the samples after cutting and polishing have been done are presented. The pictures will be shown with different magnification levels highlighting various aspects of the images.

The first two images presented figures 27 and 28 are from the S90 sample after one polishing sequence have been done. Figures 27 and 28 have a lot more detail compared with the unpolished samples from figures 20a and 20b. The increased detail makes individual carbon fibers visible and highlights the importance of removing surface roughness through polishing. However, despite increased detail the images have very little color contrast, but by adjusting brightness and polarisation carbon fiber visibility has been ensured. After this an image series from the S45 sample is presented. These are taken after size reduction of the sample. The size reduction made further polishing possible, which revealed more details in the sample. This resulted in an overall better contrast and clarity in the images (see figure 29) and allowed the stacking sequence to be observed (see figure 30). Then, in figure 31 further magnification allowed observation of a damaged carbon fiber ply right below the adhesive layer.

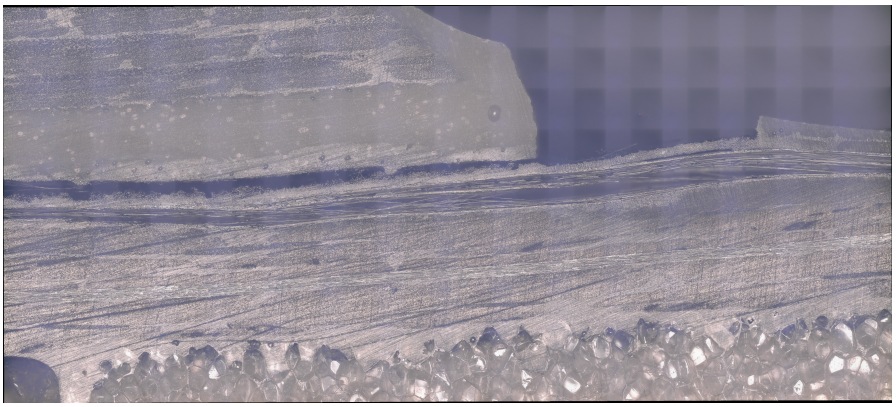

Fig. 27: Image from the S90 sample after the first polishing sequence.

Fig. 28: Image from the S90 sample after one sequence of polishing, but from a different area than figure 20b. The individual carbon fibers can be seen as bright white dots in the centre of the image and as white strands running parallel with the surface at the bottom and in the upper left corner.

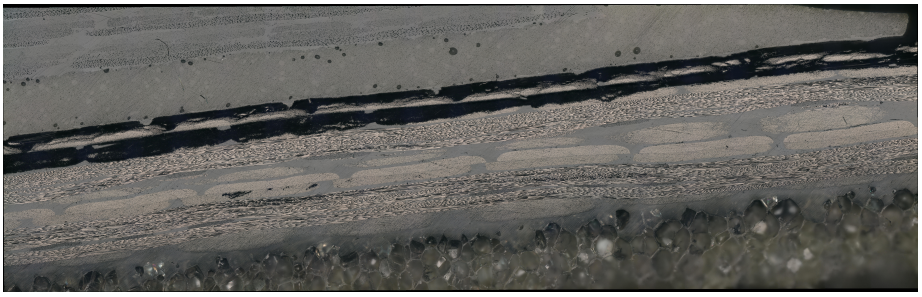

Fig. 29: Image of the S45 sample after the second and final polishing sequence. The topmost fibers of this sample is at a 45 degree angle with the examined surface, the second ply is also at a 45 degree angle with the examined surface and the three following plies are parallel with the examined surface.

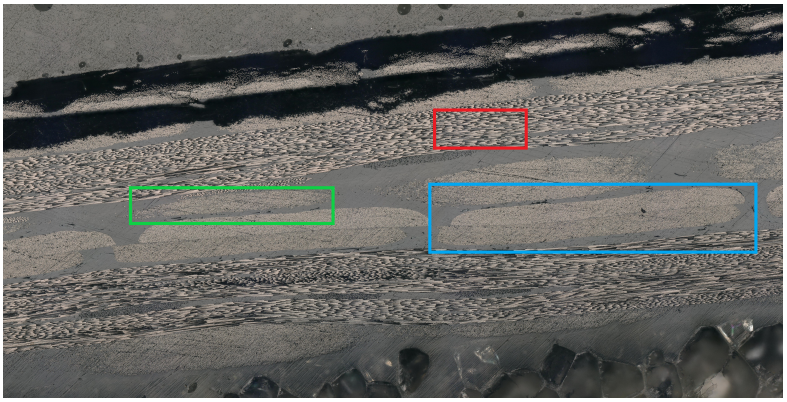

Fig. 30: The area of interest from figure 29, but magnified to show the stacking sequence more clearly. The identification of different plies has been based on figure 1 in reference [51]. The plies have three different appearances depending on the angle of the carbon fibers to the examined surface. The red rectangle shows fibers that are parallel with the examined surface, they are visible as long white bands with black dots. The green rectangle shows fibers that are at a 90 degree angle to the examined surface and are pointing straight out from the image. These fibers are visible as oval bundles of fibers surrounded by grey resin. Lastly, fibers at +- 45 degree angle to the examined surface cannot be distinguished between each other and are shown in the blue rectangle separated by a very fine line of resin. The fibers at +- 45 degree angle can be distinguished from the 90 degree fibers since their bundles are wider than those of the 90 degree fibers.

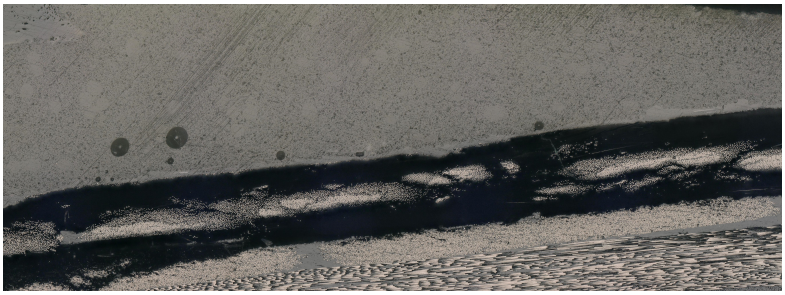

Fig. 31: S45 sample magnified even further compared with figure 30 to show how the bundles of the topmost carbon fiber ply has been fractured at several places.

The next image series is of the S90 sample with all polishing completed. In figure 32 the image quality is noticeable increased compared with figure 27 and comparable to that of figure 29. With improved image quality the carbon fiber ply sequence can again be observed in figure 33. Lastly, in figure 34 the carbon fiber ply just

beneath the adhesive layer is again observed. However, unlike in figure 31 the ply is undamaged along its length.

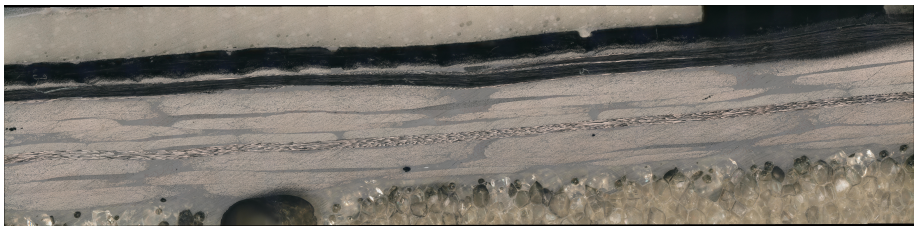

Fig. 32: S90 sample after final polishing. The topmost fibers are at a 90 degree angle with the examined surface, the second ply is parallel with the examined surface and the three following plies are at a 45 degree to the examined surface.

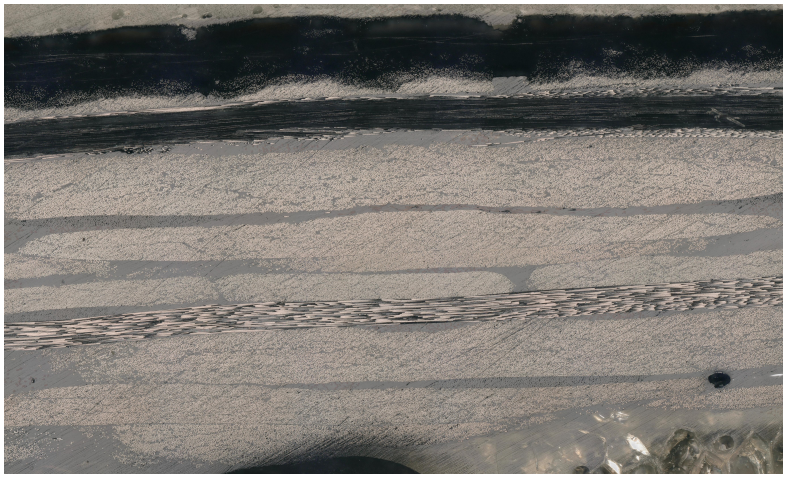

Fig. 33: Magnified version of figure 32 showing the stacking sequence more clearly. To distinguish the different plies one should use the same principles as presented in figure 30.

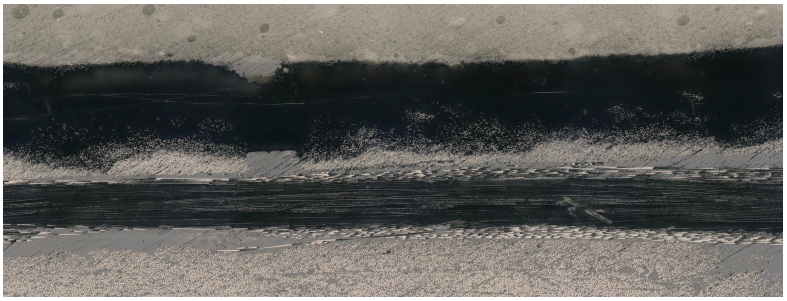

Fig. 34: S90 sample magnified even further than figure 33 to show how the bundles of the topmost carbon fiber ply has stayed together unlike the bundles from figure 31. Even the resin-rich connections between individual bundles are relatively intact.

4.2 Finite element modeling

Here images of the finite element models used will be shown along with various data. The first image (see figure 35) is the isolated carbon fiber laminate layer from the 250 mm submodel. Results from the 70 and 160 mm submodels look almost identical and are therefore excluded or reported in the appendix. Markers are placed to show the location of the element with 1 the highest tensile stress in the Z direction, 2 the highest radial tensile stress and 3 the highest RZ shear stress. These stresses play a crucial part in the fracture of the sample and their interaction was calculated in order to compare them with the failure stress of the materials in the FE model. The stress values at the marked elements and what interaction value they get can be viewed in table 4. After calculations were done, it was evident that the RZ shear stress played a minor role in sample fracture. Therefore, this value will mostly be excluded from the report. Radial stress levels are also low, but even low radial stress levels can cause cracks to appear. Furthermore, in point 2 high levels of Z stress was also observed making that point more important for the upcoming analysis.

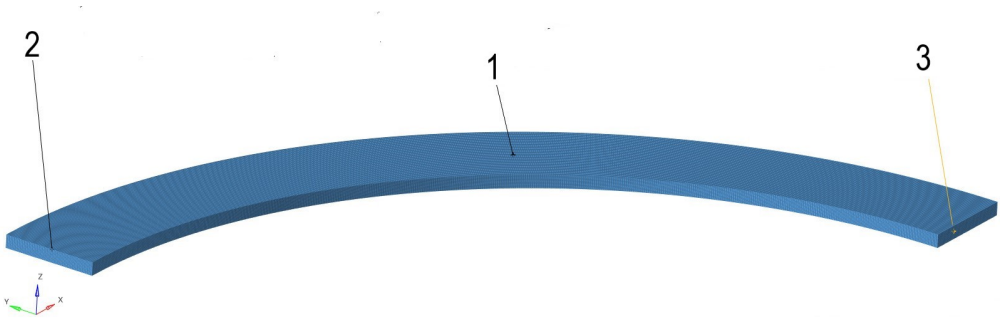

Fig. 35: Image of the 250 mm submodel where the carbon fiber laminate layer is isolated. Markers is placed at regions of interest. These markers show the location of the element with 1 the highest tensile stress in the Z direction, 2 the highest radial tensile stress and 3 the highest RZ shear stress.

In figure 36 the amplified deformation of the 250 mm model is shown to more clearly illustrate how the model deforms under load. The deformation is not shown in other images because they would be to cluttered with lines. In the next image (see figure 37) the 250 mm submodel color coded according to Z stress distribution is presented. With this an overview of the stress levels is obtained and it is clear that the highest stress is observed on the slanted edge of the glass fiber patch. However, since the failure is know to have occurred between the carbon fiber laminate and the adhesive layer that region is isolated in figure 38. In the image it can be observed how the stress in the laminate is symmetrical along the arch of the model and how it peaks at the area that runs under the edge of the glass fiber patch. More information is then gained from figure39 where the depth distribution of the stress is shown. The stress is gradually increased as one moves from the bottom and peaks at the top surface.

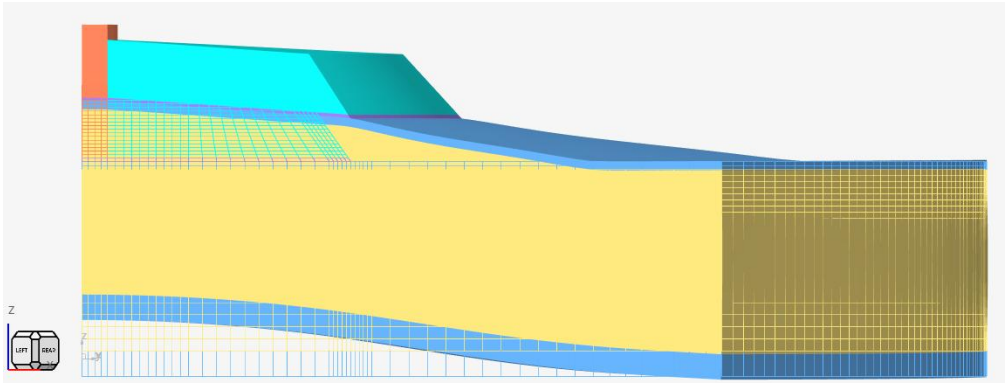

Fig. 36: The deformed 250 mm FE model after max load is applied. The deformation is amplified with a factor 5 for easier visualisation.

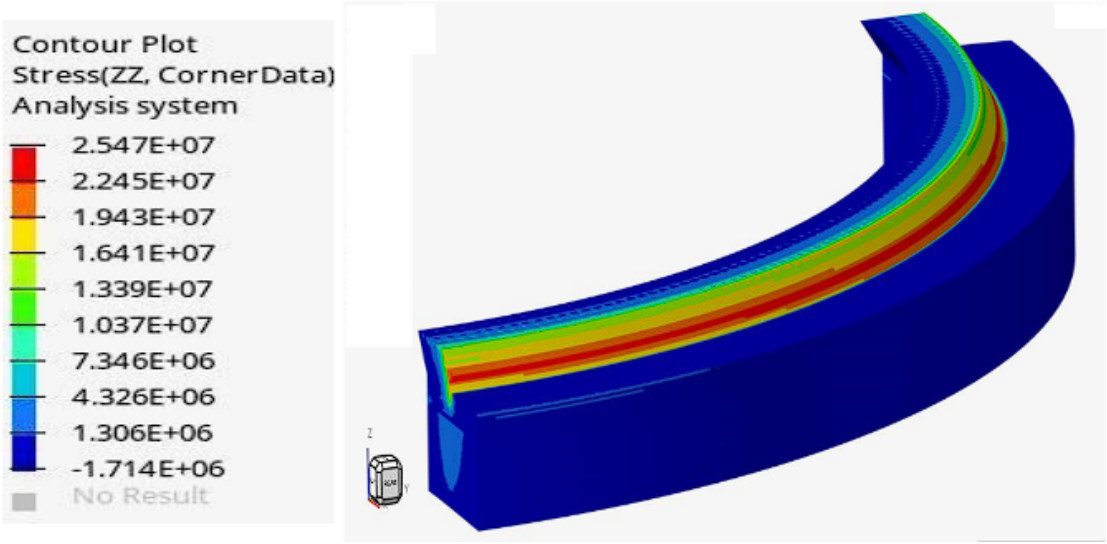

Fig. 37: Z stress distribution in the 250 mm FE submodel.

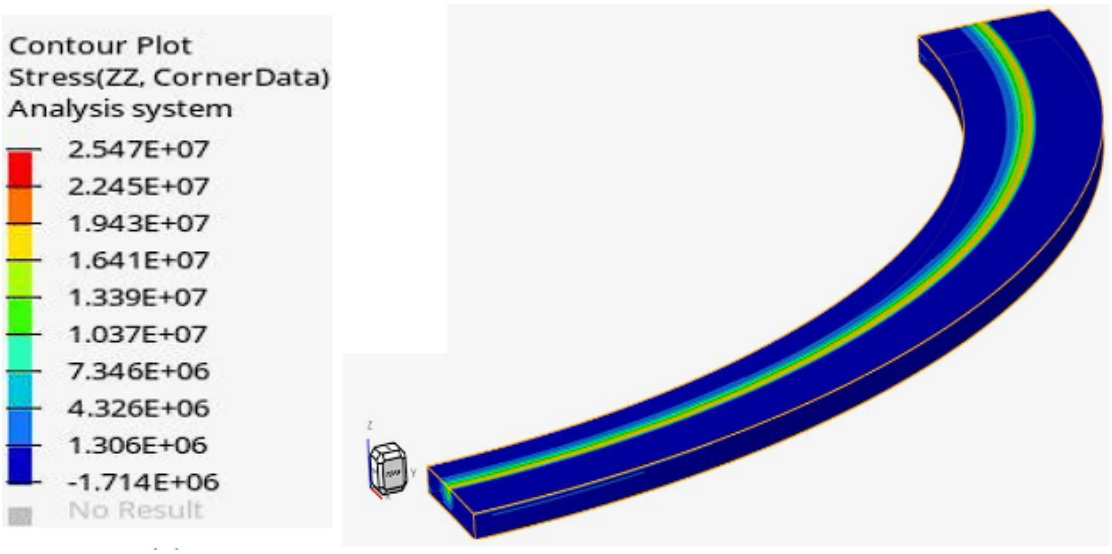

Fig. 38: Z stress distribution in the isolated carbon fiber laminate layer along the surface.

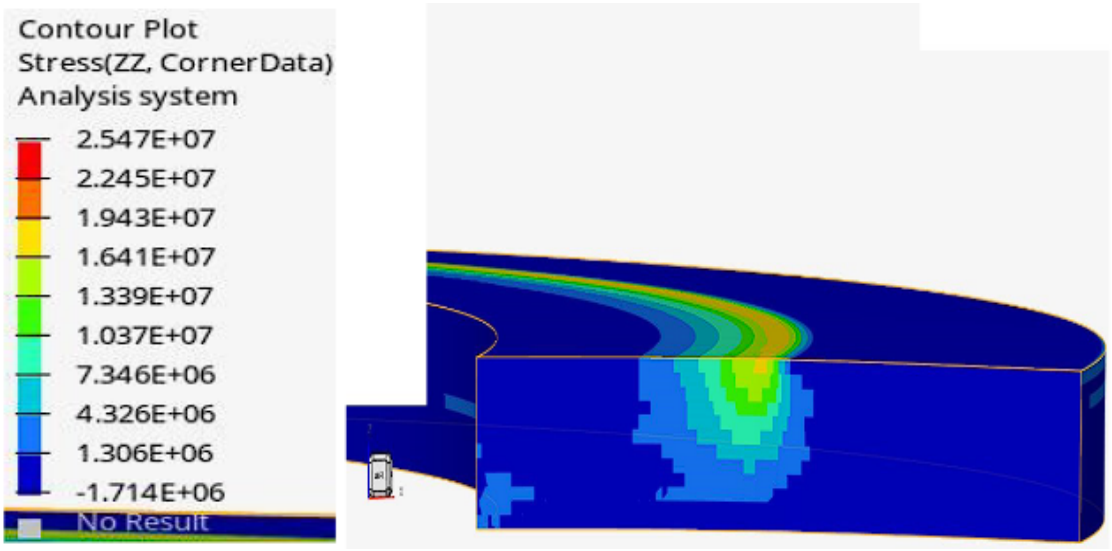

Fig. 39: Z stress distributed along the depth of the carbon fiber laminate in the 250 mm submodel.

The following image series presents the radial tensile stress in the 250 mm submodel. In figure 40 The stress is higher at one of the edges of carbon fiber laminate along the arch since the carbon fibers in the top layer at this side is parallel with the radius of the arch here. This makes the laminate stiffer in this region and thus

the stress level is higher here. In figure 41 the carbon fiber layer is isolated to show surface distribution of stress. The stress levels along the arch caused by the direction of the carbon fibers can be more clearly seen than in figure 40 . It can also be observed how the stress levels are at their peak just below the edge of the glass fiber patch. Afterwards the depth distribution of the radial tensile strength is shown in figure 42. Just below the surface the stress level drops sharply because a new laminate layer begins that has its fibers in a 90 degree angle compared with the top layer. So if the other edge of the arch would have been observed the picture of the two topmost layers would basically be reversed but with different levels.

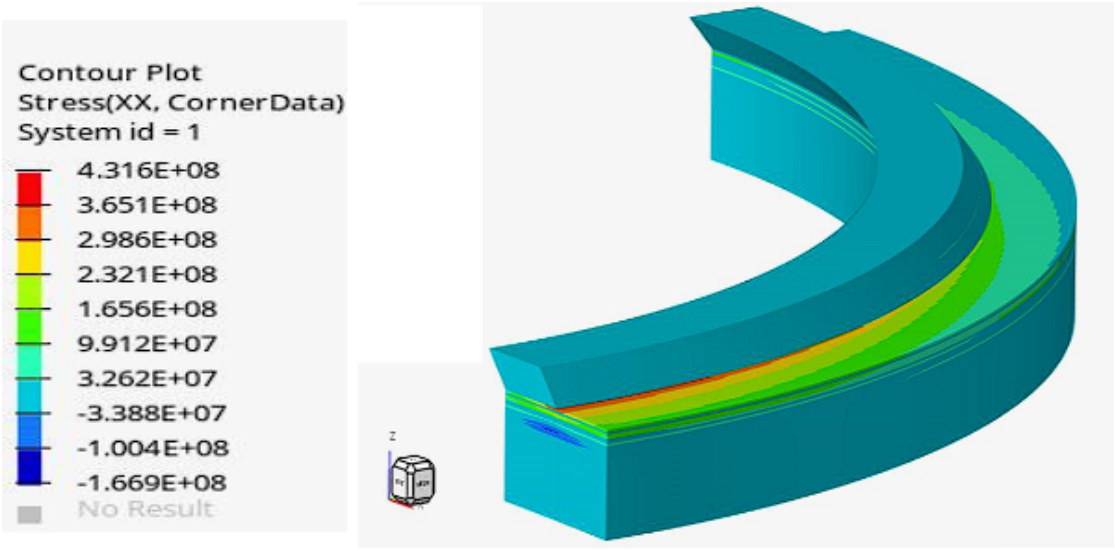

Fig. 40: Radial tensile stress distribution of the 250 mm FE submodel.

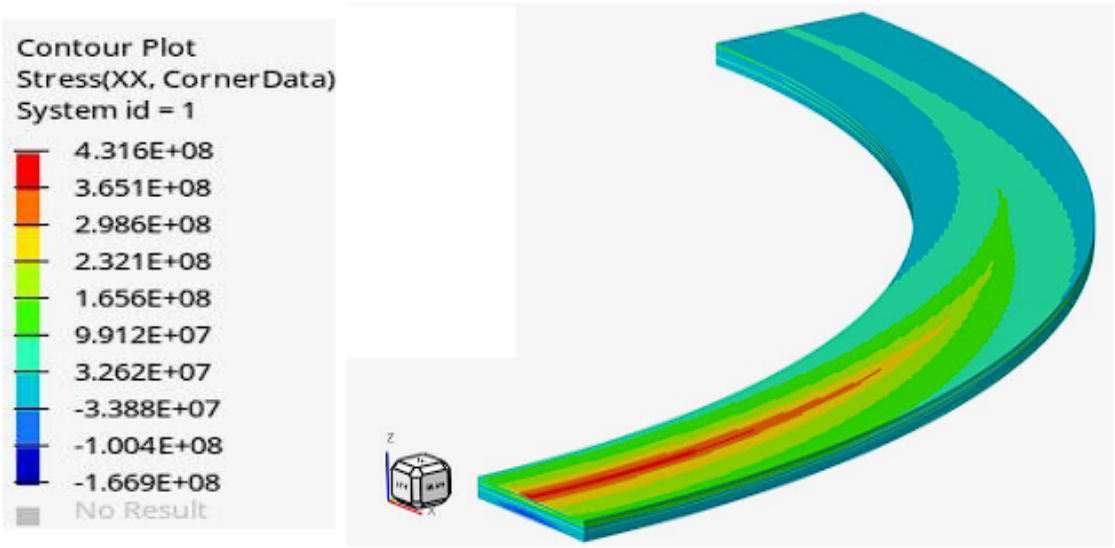

Fig. 41: Radial tensile stress distribution along the surface of the carbon fiber laminate.

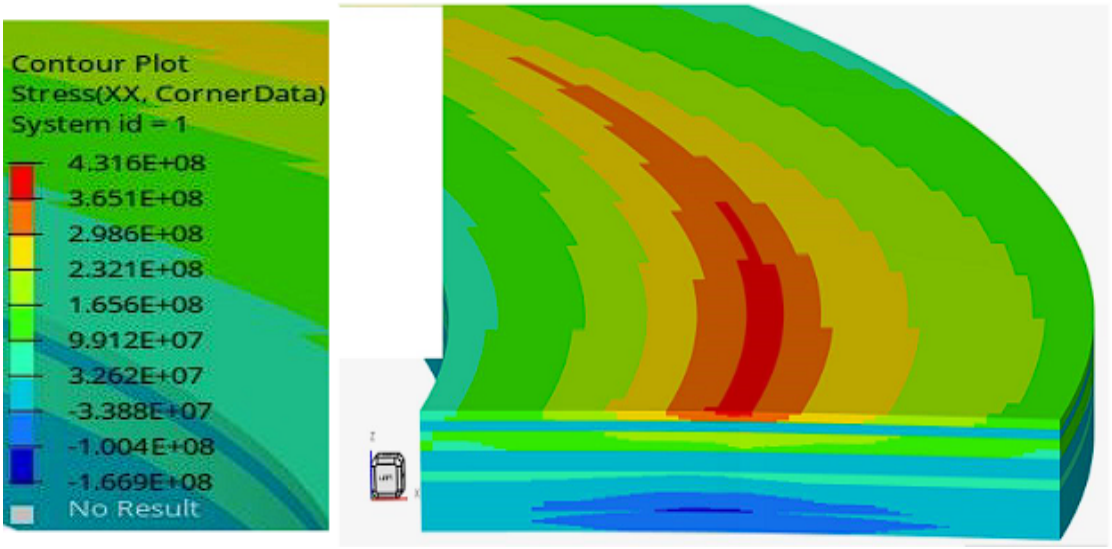

Fig. 42: Radial stress distributed along the depth of the carbon fiber laminate in the 250 mm submodel.

Lastly, the peak stress values and the calculated interacting failure values of the 70, 160 and 250 mm submodels are shown in table 4. The ultimate strengths that have been used for the ratios in the interacting failure criteria is 15 MPa for stress in the Z direction, 25 MPa for the RZ shear stress and 1400 MPa for the radial

tensile strength in the fiber direction. The radial tensile stress strength is based on the rule of mixtures with a fiber content of 50% and is only valid in the fiber direction. The strength in shear direction is based on the minimum requirement from Kockums at 15 MPa, but according to their tests the strength of the carbon fiber laminate in Z direction is about 15-17 MPa.

Table 4: Different stress values in all the positions of interest across all the sub-models and their interacting stress value calculated using equation 3.

-	σ_z $[MPa]$	$\sigma_r z$ $[MPa]$	$\sigma_r ts$ $[MPa]$	Interacting matrix stress failure criteria value
Submodel 250 position 1	18.86	-13.18	183.38	1.37
Submodel 250 position 2	16.18	-10.62	431.63	1.20
Submodel 250 position 3	0.98	-19.85	-46.84	0.8
Submodel 160 position 1	17.23	-11.08	230.70	1.24
Submodel 160 position 2	16.89	-11.11	389.85	1.24
Submodel 160 position 3	2	-18.33	-43.34	0.75
Submodel 70 position 1	14.63	-9.72	54.08	1.05
Submodel 70 position 2	14.32	-10.35	272.57	1.06
Submodel 70 position 3	2.27	-15.36	-36.05	0.63

5 Analysis and discussion

5.1 Anlysis failure mechanisms from experimental results

The purpose of the microscopic examination was to compare it with the results from the FE analysis, but they might also show phenomenons outside of the narrow scope given by FE modeling.

The S45 and the S90 samples are very similar (figure 29 and 32). No damage is seen in the foam layer and the glass fiber layer and almost no damage can be seen in the adhesive layer and only the upper parts of the carbon fiber laminate is visibly damaged. This is expected, because in previous images such as figure 8b and in descriptions of test samples, the uppermost 1 or 2 layers of the carbon fiber laminate delaminated. In some cases, parts of the carbon fiber layer also detached from the adhesive layer. Looking at the image 30 and 33 there seems to be a difference in the size of the gap created by the delamination in the S45 and S90 samples. Nevertheless, the gap size is believed to be affected by sample preparations and not by the delamination during fracture.

An important phenomenon is that the fiber bundles in the topmost ply in the S45 sample are fractured (see figure 31) while the top ply of the S90 sample is held together even in between the fiber bundles in the resin rich areas (see figure 34). The explanation for this is believed to be higher stress concentrations in the S45 compared with the S90 sample. The increased stress concentration in the S45 sample arises from the fact that both of the top plies are at a 45 degree angle to the examined surface, this gives the laminate a lower bending stiffness in this area and can be seen in figure 43. Below the top two layers follow three layers that are parallel with the examined surface, two that together make the UL ply and the lowest of these three that is the upper part of the BLT ply. Since all of these layers are in parallel with the examined surface it gives them the highest possible bending stiffness. This difference in bending stiffness between the top two plies and the three plies below is assumed to cause larger deformations in the top two plies compared with the 3 plies beneath them, which increases the risk of delamination. This extra vulnerability to delamination has likely caused the fracturing of the fiber bundles in the S45 sample by shearing them in the resin region between fibers. Therefore, the fracturing of the fiber bundles in the S45 sample is seen as an indication that deformations are actually larger in this direction. Thus, it is also likely a point where cracks and delamination start. Moreover, this also indicates that the fracturing of the laminate is because of matrix cracks that leads to a matrix failure.

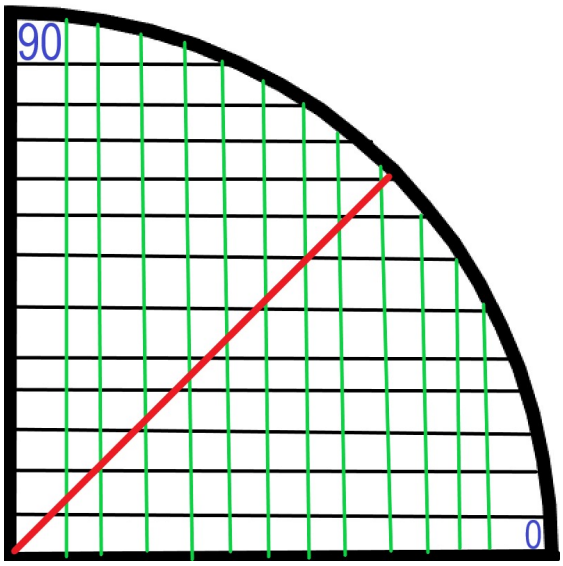

Fig. 43: Schematic of the model used in the FE analysis. The black lines indicate the direction of the carbon fibers in the topmost ply, while the green lines indicate the direction of the fibers in the second ply. The blue numbers indicate degrees. The red line is at a 45 degree angle to the fibers in the two topmost plies. Along this red line the S45 sample has been cut and this is also the direction where the combined stiffness of the top two plies is at their lowest. Thus, this line also indicates the direction where matrix cracks while be most severe and where the sample will fracture.

5.2 Anlysis of FE modeling results

As can be seen from table 4 (which is based on the different stresses from the pointed out elements in figure 35 and corresponding elements in the 160 and 70 submodels), all the FE models reach a value of 1 or above in at least 1 out of 3 elements. This means that the interaction of all three different stresses that has been investigated is enough to fracture the carbon fiber laminate in this area. Since the models are exposed to the same global load that managed to fracture real physical samples with the same dimensions, this indicates that the FE model corresponds well with the physical experiments.

Nevertheless, one might question why the samples are loaded to the point where several elements exceeds a value of 1, especially since debonding is not included in this FE analysis. The reason for this is that the load used is equal to the one used during mechanical testing. At the same time the failure criteria in the FE analysis is based on minimum strength values for specimens as is standard. Therefore, it is to be expected that some elements reach values above 1 since a random

sample should require more load to fracture than the minimum value. This is not optimal, since the behaviour of the elements past a value of 1 is most likely not very accurate. Although, this might also be a way of working around the simplicity and inaccuracy of the model. Because, the load to fracture the samples is known, and it is clear that this causes elements to reach values higher than 1. Thus, if the modeling had been done so that the elements simply reached a value of 1, the fracture load would be underestimated with the current model. Therefore, in order to use the more appropriate load scenario where the elements reache a value of 1, a more detailed FE model will have to be used. Alternatively, debonding should be included in the model so that the failure criteria can be based on minimum values and still be accurate for other specimens when their elements reach values above 1.

There is however more information to be found from table 4 and the figures. The element with the highest shear stress does not reach a value of 1, but at most reaches a value of 0.8. The reason for this is that the out of plane stress and the radial stress is much lower in these elements, which can be seen from table 4, and the shear stress is not even close to its limit. As such, even though the XZ shear stress interacts positively with the other stresses, so that failure can be observed before their individual strength limits are reached, it is comparatively unimportant.

The radial tensile stress was mainly investigated because of the damage build up in fiber composites that occurs far away from the strain limits of the individual components in the composite. The highest stress level reached, about 430 MPa, is far lower than the calculated fracture stress at 1400 MPa. The carbon fibers that are part of the laminate in the examined samples is Toray T700S fibers. They have a strain at failure of 2.1% and tend to yield right before ultimate failure, so the behavior across almost the whole strain span is elastic. The vinyl ester matrix has a strain at failure of 5.2%. Nonetheless, carbon fiber composites made of these components begin exhibiting damage in the form of micro cracks already at 0.4% strain. This damage was observed in fibers with a 90 degree angle to the pulling direction. In the examined samples, the two topmost plies of carbon fibers are at a 90 degree angle to each other, so this type of damage might then be relevant to the FE models of this report. The radial stress level in the 250 mm model causes a strain of 0.37% if the rule of mixture is used to calculate the stiffness of the composite, so some micro cracks might very well form. On the other hand, this initial damage only affects the stiffness of the carbon fiber composite by about 2%, so in the short term it might not be crucial if 0.4% strain is reached. However, these micro cracks could act as initiation sites for larger cracks and if more long term testing or modelling is conducted, then initial small damage might

be more relevant because of its synergistic effects with the other stresses and due to damage accumulation. Additionally, the location of the element with the highest radial tensile stress is on one of the faces at the end of the arch parallel to the X (0 degrees) or Y axis (90 degrees). This is also expected because at these positions one of the two topmost carbon fiber plies has its fibers parallel to the surface. This in turn means that the ply is most stiff in the radial direction at these locations and therefore, due to stress shielding, the highest radial tensile stress will be observed at one of these locations.[52]

Now we need to consider the out of plane stress that causes delamination due to mode 1 fracture (see figure 10). In this direction, the carbon fiber has the lowest strength limit at about 15-17 MPa, which follows theory regarding fracture modes, which states that the mode 1 fracture requires the least amount of energy. So, because of that, this type of stress is suspected to be the most crucial in determining if the sample fails or not. This is further confirmed by looking at the FE results. Since in the 250 and 160 mm submodels there are elements where the out of plane stress exceeds 17 MPa. Thus, failure is caused before even considering the other two types of stress. The outlier among the FE results is the 70 mm submodel which has an out of plane stress below 15. However, when the other types of stress are considered, the model does indicate that a sample would fail at the element which has the highest out of plane stress. Nevertheless, the 70 mm model is slightly less detailed than the other two models and this is believed to be the reason why the stresses are lower in this model. The sensitivity of this FE method to the mesh density is in accordance with literature on the subject. As for the positions of these elements, they are at an approximate 45 degree angle to the X axis for both the 250 and 160 mm model. This is again not surprising because the stiffness in this region is at its lowest since both the two carbon fiber plies at the top have their fibers at a 45 degree angle to the radial direction. Moreover, at least one ply with fibers that are parallel to the radial direction are below these two plies, which concentrates the deformation to the two top plies. This in turn causes them to bend more, and this corresponds to higher out of plane stress. The 70 mm model does not follow this trend but rather has the element with the highest out of plane stress at a 60 degree angle. No explanation to this has been found except the fact that the model is less detailed. Nevertheless, it seems unlikely that the lower mesh density would cause the element with maximum out of plane stress to show up elsewhere on the submodel.[53]

5.3 Correlation between experimental and FE modeling results

Both the results from the microscopic analysis and the FE results can be improved, but together their predictive power is substantially increased. To show this one can look at the elements chosen to be investigated and their stress values used with equation 3. According to table 4, it is clear that the element with the highest shear stress does not seem to be in the location where failure starts. But both the elements with the maximum out of plane stress and the element with the highest radial tensile stress surpass the strength limit in all of the models. On the other hand, the microscopic results indicate that the sample would fail first at a position that is in a 45 degree angle to the topmost fibers, which corresponds with the position of the element with the maximum out of plane stress in the 250 mm submodel derived from the examined samples.

The physical samples provide a more broad analysis compared with the FE model and has shown that there is not only delamination of the carbon fiber laminate, but the carbon fiber laminate also detaches from the adhesive. Which of these occurrences that happens first is not clear, but what is clear is that the carbon fiber laminate at least partially detaches from the adhesive (see figure 8b). This combined with the fact that FE model is very simplified, it does not feature plasticity, defects or the wavy pattern of the carbon fiber layers, means that the microscope images hold more weight in this analysis. Thus, the most likely area where the matrix cracks might become catastrophic would be close to the edge of the glass fiber patch at 45 degree angle to the two top carbon fiber plies.

5.4 Further and alternative work that can be done

With the results analyzed and discussed, the next step would now be to reflect on what can be done in the future. Both the microscopic analysis and the FE modeling can be improved with more statistical data. In other words the microscopic analysis of more samples and of samples with different patch sizes, core densities and carbon fiber laminate thicknesses together with FE modeling of these samples would give more certainty to the results.

Something that would be very useful but a bit hard to perform would be to examine a sample during the actual tensile testing that causes the fracture of the sample. If an optical microscope were to be used, the specimen that is tested would have to be cut so that a surface where the interface between the carbon fiber laminate and adhesive is visible. However, to cut the specimen in this way would most likely affect the strength substantially. If one instead looks beyond the capabilities of optical microscopy, there are other techniques that could be used to gain information

on the specimen while it is being tested. Digital image correlation (DIC) uses a camera and computer software to connect visual data to local strain levels in the specimen that can then be used to give the FE simulations more data to improve them. DIC howeve, needs line of sight with the area that is to be examined. This limitation could be overcome by other techniques such as synchrotron computer tomography.

When it comes to the FE modeling, the first step would be to not model materials like the adhesive as linear elastic and to include plasticity in the model. At least the inclusion of plasticity and non-linearity of the adhesive would reduce stress concentrations in the model since materials would yield and lose stiffness as they approach their failure strength. Lower stress concentrations could make the results less conclusive since the maximum stress observed in the model would decrease and thus the values of table 4 would be closer to 1 or even below 1, which means that failure would seem less certain. On the other hand, plasticity may shift the importance of the three investigated stress types and could thus reveal another area where failure would occur. Plasticity might also, through the more even distribution of stresses, reveal a larger area where the strength limit is surpassed, making failure of the whole specimen more likely. So, if the inclusion of plasticity decreases the peak stress from 1.3 times the strength limit to 1.1, but at the same time doubles the affected area, a failure would probably be more likely despite the lower peak stress. Furthermore, the potential lower peak stress due to plasticity could be increased if one models defects and the damage that starts appearing during testing.

A couple of other interesting factors that could be investigated without changing the model too much would be to vary the thickness of the adhesive layer or to change the adhesive. These factors proved rather hard to include in this report because literature on the subject of adhesive thickness was not very conclusive. Additionally, the nature of the fracture was not clearly understood in the beginning of this report. However, it is known now that stress concentrations seem to be the reason for failure, a thicker adhesive layer could be one way of reducing stress concentrations and would thus be very relevant parameter to model. Furthermore, a rather lengthy discussion was held in section 2.2.4 and 2.2.5 on how the chemistry of the adhesive might affect bond strength. However, with the clear goal to reduce stress concentrations changing the adhesive becomes more simple. Since, to combat this problem, another epoxy adhesive could be chosen that would have a similar chemistry as the current adhesive, but a lower stiffness and larger strain at failure. With these changes to the adhesive, the stress concentrations in the adhesive joint would likely decrease just like if the thickness was increased.

A change that would be more substantial is to base the model on fracture mechanics

and virtual crack closure techniques or energy release rate. This modeling technique promises to remove weaknesses such as dependence on the mesh size in the areas of interest and could give more accurate results. This modelling technique could be done with cohesive zone elements which can handle debonding, so that areas where the strength limit is surpassed stops increasing their stress levels. This in turn would decrease stress concentrations and result in a more accurate modeling. Another FE modeling technique is based on representative volume elements (RVE) which can provide detailed results that not only answers if and why a fracture happens, but also how it happens.

There is certainly a lot of future work to be done. However, in defense of the work already carried out, Kockums uses a safety factor of 3 when designing structural elements made out of composite materials. So, the results they need do not have to be overly detailed or accurate. They are also initially more interested in knowing if failure occurs rather than why or how it happens. Lastly, all the alternative techniques mentioned above would require more time and resources, which further justifies the more simplistic approach taken in this thesis work.

Conclusion

In this report a FE model was established where three different stress types were investigated. These were deemed crucial to determining the strength of the matrix dominated failure in the adhesive joint between a glass fiber patch and carbon fiber sandwich panel. These stresses were then used in an interaction criteria to calculate if failure would occur.

The FE results indicate that failure would occur in the top carbon fiber ply thus agreeing with the mechanical results. Optical microscopy was used for further failure analysis. The images from the microscope largely confirmed the results of the FE modeling in that the top carbon fiber ply fail first and that the fracture started, approximately at a 45 degree angle to the radial direction of the model and to both of the topmost carbon fiber plies. However, the micrographs also reveal that the top carbon fiber ply detach from the adhesive.

Since the developed FE model agrees with mechanical tests and with the microscopy results, it is believed to have some predictive power. Thus, the FE modeling is considered to have fulfilled its purpose of predicting failure in the adhesive joint between the glass fiber patch and the carbon fiber sandwich panel and its purpose of acting as basis for further and more detailed FE modeling.

The conclusion is therefore, that samples fracture in the topmost carbon fiber laminate layers where the carbon fibers are at a 45 degree angle to the radius of the sample and where the out of plane stress is at its maximum. So, ship designers is recommended to use the local maximum out of plane stress as their limiting design parameter.

References

[1] Wikipedia, "Specific strength." https://en.wikipedia.org/wiki/Specific_strength. Last accessed 10 March 2022.

[2] M. Keegan, D. Nash, and M. Stack, "Modelling rain drop impact of offshore wind turbine blades," vol. 6, p. fig 5, 06 2012.

[3] E. Britannica, "The steamboat." https://www.britannica.com/technology/ship/The-steamboat. Last accessed 10 July 2022.

[4] E. Britannica, "The atlantic ferry." https://www.britannica.com/technology/ship/The-Atlantic-Ferry. Last accessed 10 July 2022.

[5] E. Britannica, "Cargo ships." https://www.britannica.com/technology/ship/Cargo-ships. Last accessed 10 July 2022.

[6] B. BOON, "What limits the dimensions of wooden ships? from naval gigantism of chinese ming dynasty to universal physics in a seaway." https://www.academia.edu/33216498/WHAT_LIMITS_THE_DIMENSIONS_OF_WOODEN_SHIPS_From_naval_gigantism_of_Chinese_Ming_Dynasty_to_universal_physics_in_a_seaway, 04 2008. Last accessed 10 March 2022.

[7] F. Campbell, *Adhesive Bonding and Integrally Cocured Structure*, pp. 241–301. 12 2004.

[8] Y. K. Kumar and D. Lohchab, *Influence of Aviation Fuel on Mechanical properties of Glass Fiber-Reinforced Plastic Composite*. PhD thesis, 05 2016.

[9] A. Mouritz, E. Gellert, P. Burchill, and K. Challis, "Review of advanced composite structures for naval ships and submarines," *Composite Structures*, vol. 53, pp. 21–42, 07 2001.

[10] E. Britannica, "Composite material." https://www.britannica.com/technology/composite-material. Last accessed 10 March 2022.

[11] Australian Academy of Science, "The science and technology of composite materials." https://www.science.org.au/curious/technology-future/composite-materials. Last accessed 10 March 2022.

[12] T. Megson, *Chapter 11: Materials*, ch. 11, pp. 397–419. Butterworth-Heinemann, 08 2021.

[13] D. Tam, S. Ruan, P. Gao, and T. Yu, "High-performance ballistic protection using polymer nanocomposites," *Advances in Military Textiles and Personal Equipment*, pp. 213–237, 07 2012.

[14] E. Britannica, "Fibreglass." https://www.britannica.com/science/plastic/Foaming. Last accessed 10 July 2022.

[15] CompositesWorld, "Materials processes: Resin matrices for composites." https://www.compositesworld.com/articles/the-matrix. Last accessed 10 March 2022.

[16] E. Gamstedt and L. Berglund, "Fatigue of thermoplastic composites," *Fatigue in Composites: Science and Technology of the Fatigue Response of Fibre-Reinforced Plastics*, pp. 314–338, 10 2003.

[17] L. Iannucci, *Design of Composite Ballistic Protection Systems*, pp. 308–331. 12 2017.

[18] D. M. M.F.S.F., *Interaction of matrix cracking and delamination*, pp. 327–343. 12 2008.

[19] Y. K. Kumar and D. Lohchab, *Influence of Aviation Fuel on Mechanical properties of Glass Fiber-Reinforced Plastic Composite*. PhD thesis, 05 2016.

[20] C. E. Ueng, *Encyclopedia of Physical Science and Technology (Third Edition)*, pp. 407–412. 06 2003.

[21] S. Lathabai, *Joining of aluminium and its alloys*, pp. 607–654. 11 2010.

[22] K. L. Devries and D. Adams, "Mechanical testing of adhesive joints," *The Mechanics of Adhesion*, pp. 193–234, 12 2002.

[23] S. Ebnesajjad and C. Ebnesajjad, *Chapter 5. Theories of Adhesion*, pp. 77–92. 12 2006.

[24] Huntsman, "Araldite® 2015-1." https://www.intertronics.co.uk/wp-content/uploads/2015/12/ara2015.pdf. Last accessed 10 March 2022.

[25] J. White, "Polymer ageing: Physics, chemistry or engineering? time to reflect," *Comptes Rendus Chimie - C R CHIM*, vol. 9, pp. 1396–1408, 11 2006.

[26] A. Rudawska, "The effect of the salt water aging on the mechanical properties of epoxy adhesives compounds," *Polymers*, vol. 12, p. 843, 04 2020.

[27] A. Le guen geffroy, p. y. le gac, B. Habert, and P. Davies, "Physical ageing of epoxy in a wet environment: Coupling between plasticization and physical ageing," *Polymer Degradation and Stability*, vol. 168, p. 108947, 08 2019.

[28] Wikipedia, "Epoxy." https://en.wikipedia.org/wiki/Epoxy. Last accessed 10 March 2022.

[29] A. Kandelbauer, G. Tondi, O. Zaske, and S. Goodman, *Unsaturated Polyesters and Vinyl Esters*, pp. 111–172. 01 2014.

[30] M. Vuksanovic and R. Jancic Heinemann, *Micro and nanoscale morphology characterization of compatibilized polymer blends by microscopy*, pp. 299–330. 01 2020.

[31] N. Nasri, "Effect of an adhesive layer on the mode i delamination in unidirectional cfrp bonded joints," 2017.

[32] M. Rośkowicz, J. Godzimirski, A. Komorek, and M. Jasztal, "The effect of adhesive layer thickness on joint static strength," *Materials*, vol. 14, p. 1499, 03 2021.

[33] N. Saba, M. Jawaid, and M. Sultan, *An overview of mechanical and physical testing of composite materials*, pp. 1–12. 01 2019.

[34] D. Ruan, M. Kariem, and I. Crouch, *High Strain Rate and Specialised Testing*. 09 2016.

[35] Huntsman, "Araldite® 2015-1." `https://www.huntsman.com/products/araldite2000/araldite-2015-1`, note = Last accessed 10 March 2022,.

[36] Z. Jia, D. Hui, G. Yuan, J. Lair, K. t. Lau, and F. Xu, "Mechanical properties of an epoxy-based adhesive under high strain rate loadings at low temperature environment," *Composites Part B: Engineering*, vol. 105, 08 2016.

[37] Huntsman, "Araldite® 2014-2." `https://www.huntsman.com/products/araldite2000/araldite-2014-2`. Last accessed 10 March 2022.

[38] M. Carter and J. Shieh, "Guide to research techniques in neuroscience," *Guide to Research Techniques in Neuroscience*, pp. 117–144, 01 2010.

[39] Wikipedia, "Electron microscope." `https://en.wikipedia.org/wiki/Electron_microscope`. Last accessed 8 June 2022.

[40] D. Grubb, *2.17 - Optical Microscopy*, pp. 465–478. 6 2012.

[41] Keyence, "Stereoscopic microscopes." `https://www.keyence.com/ss/products/microscope/microscope_glossary/optical_microscopes/stereoscopic_microscope.jsp`. Last accessed 8 June 2022.

[42] Wikipedia, "Polarization (waves)." `https://en.wikipedia.org/wiki/Polarized_light_microscopy`. Last accessed 29 May 2022.

[43] B. Rapp, *Chapter 32 - Finite Element Method*, pp. 655–678. 12 2016.

[44] Elinder, Joel, "Improving comfort simulations of sleeping mattresses for IKEA." http://lup.lub.lu.se/student-papers/record/9015683, 2020. Student Paper.

[45] E. Barbero, *Introduction to Composite Materials Design*. 07 2010.

[46] A. Pramanik, A. Basak, Y. Dong, P. Sarker, M. Uddin, G. Littlefair, A. Dixit, and S. Chattopadhyaya, "Joining of carbon fibre reinforced polymer (cfrp) composites and aluminium alloys-a review," *Composites Part A: Applied Science and Manufacturing*, vol. 101, pp. 1–29, 06 2017.

[47] Diabgroup, "Technical data divinycell h." https://www.diabgroup.com/media/eyajkrhd/diab-divinycell-h-february-2022-rev21-si.pdf. Last accessed 26 July 2022.

[48] Toray, "T700s standard modulus carbon fiber." https://www.toraycma.com/wp-content/uploads/T700S-Technical-Data-Sheet-1.pdf.pdf, note = Last accessed 26 July 2022,.

[49] JPS, "E-glass s-glass." https://jpscm.com/products/e-glass-s-glass/. Last accessed 26 July 2022.

[50] Reichhold, "Dion® 9102 series bisphenol-epoxy vinyl ester resins." https://reichhold.com/documents/1499_DION9102SERIES.pdf. Last accessed 26 July 2022.

[51] L. Asp, E. Marklund, J. Varna, and R. Olsson, "Multiscale modelling of non-crimp fabric composites," vol. 3, 11 2012.

[52] F. Edgen, D. Matsson, L. E. Asp, and Varna, "Formation of damage and its effects on non-crimp fabric reinforced composites loaded in tension," *Composite Structures*, vol. 64, pp. 675–692, 2004.

[53] M. Jamal Omidi and M. Mohammadi Suki, "Investigation of defect effects on adhesively bonded joint strength using cohesive zone modeling," *Journal of Mechanical Engineering*, vol. 68, pp. 5–24, 11 2018.

Appendix

Here in the appendix a couple of figures are included that are rather similar to some of the figures in the results section and was thus deemed superfluous. However, the figures are included here for the interested reader.

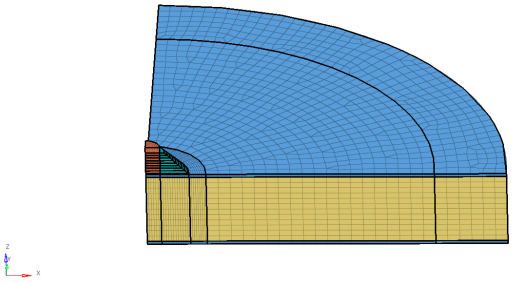

Fig. 44: An overview of the FE model which has a patch with a diameter of 70 mm. The blue components is carbon fiber laminate, red is the stainless steel insert, yellow is the PVC core and teal represents the glass fiber patch.

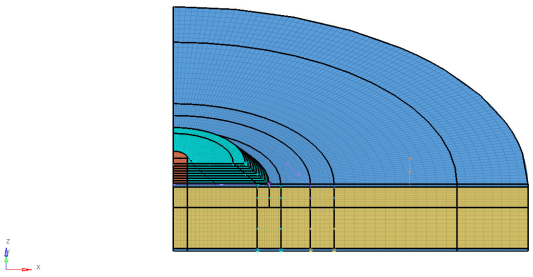

Fig. 45: An overview of the FE model which has a patch with a diameter of 160 mm. The blue components is carbon fiber laminate, red is the stainless steel insert, yellow is the PVC core and teal represents the glass fiber patch.